

1

Fundamental Concepts

Readers of this book are assumed to have some knowledge of the fundamental concepts that underlie the elaborate mathematical structure of quantum mechanics. Nevertheless, a recapitulation of these basic ideas is in order here. Introductory treatments take the beginner to base camp, and for good reason do not raise issues that can be postponed safely until demanding climbing is about to start. That is to come, however. For that reason, this review of the fundamentals will include some discussion of the role of relativity in quantum mechanics, why consistency imposes non-classical conditions on the electromagnetic field, and fundamental features of quantum mechanics that are only revealed by multi-particle states:

1.1 Complementarity and Uncertainty

With the wisdom of hindsight, today one can say that certain qualitative features of nature, apparent well before Planck and Einstein invented quantization, posed profound enigmas for the conceptual structure of classical physics. One example will suffice to make this point.

According to the equipartition theorem of classical statistical mechanics, the specific heat of a gas is proportion to the number of degrees of freedom N_f of the individual molecules that compose the gas. If the gas is noble, with apparently structureless constituents, the straightforward count would give $N_f = 3$ for the translational degrees of freedom, which agrees with experiment at all but low temperatures. But even a 19th-century skeptic could ask why this is credible, for if the atoms are structureless, how can they display an excitation spectrum — can a structureless piano play a sonata? Furthermore, according to classical statistical mechanics, the degrees of freedom that generate the excitation spectrum must be included at all temperatures in calculating the specific heat, and this would destroy the agreement with experiment.

The classical *Weltanschauung* leads to whole array of profound puzzles. To give just one other example, it cannot explain why the properties of a sample of an element are identical to that of *any other* sample of the same element, irrespective of their prior chemical and physical history — whether one sample had been extracted from one compound and another from a different compound, by totally different methods. Such puzzles, recognized by only a handful before 1900, were removed by the hypothesis that energy is quantized. With this assumption, it no longer matters that the molecules have electronic, nuclear, and even subnuclear modes of excitation if the gas in which the molecule finds itself is at room temperature, for then the naive count of N_f is correct because the internal degrees of freedom are effectively frozen out. Should the molecule be at the center of the sun, however, that

count would be deeply wrong because then it would dissociate into its electrons and nuclei, and these separate constituents would react with the surrounding matter.

(a) Complementarity

That quantization of energy is incompatible with classical mechanics was obvious and distressing to Planck from the start. In the following quarter century, it became increasingly clear that quantization in any guise could not be grafted onto classical mechanics or electrodynamics — that a fundamentally new theory was necessary because classical physics could not even provide a language for describing a host of atomic phenomena in purely qualitative terms. This theory — quantum mechanics and quantum electrodynamics — would have to lead logically from basic assumptions to quantization of such quantities as energy and angular momentum, and also incorporate atomic phenomena with continuous energy spectra, such as collisions. And the new theory would have to satisfy Bohr's *correspondence principle* — loosely speaking, reduce to classical mechanics and electrodynamics in the limit of large quantum numbers. How experiment and theory combined to give birth to quantum mechanics and electrodynamics is a fascinating story that is beyond the scope of this book; brief remarks about this history and subsequent developments, and some references to the original literature and to historical studies, can be found at the end of this chapter, and in chapter 13.

The study of the interaction between light and matter provided most of the crucial clues in the historical development of the quantum theory, and still offers a fairly direct path to central concepts of quantum mechanics and electrodynamics. To be specific, consider the Compton effect, which emerges from the scattering of γ -rays by electrons. Classical electrodynamics would describe the incident γ -ray as a nearly monochromatic wave packet of mean wave vector \mathbf{k} , and claim that its energy and momentum are proportional to the square of the field strength.¹ This field would force the electrons to oscillate with frequency $\omega = ck$, and the acceleration of the charge would produce an outgoing ("scattered") electromagnetic wave having the *same* frequency and wavelength as the incident radiation, and an angular distribution that is roughly dipolar. After the collision, classical physics would say that the electron would acquire a momentum along \mathbf{k} if it had been at rest initially.

The experiments of Compton and his followers gave results in striking disagreement with these predictions. Most, but not all, of their results could be accounted for by accepting Einstein's photon concept: that the electromagnetic wave is to be viewed as an assembly of massless particles, *photons*, each carrying an energy and momentum given by

$$E = \hbar\omega, \quad \mathbf{p} = \hbar\mathbf{k}, \quad \hbar \simeq 1.054 \times 10^{-27} \text{ erg sec}, \quad (1)$$

where \hbar is Planck's constant. By treating the process as a collision between a massless photons and an electron of mass m obeying the relativistic laws of energy and momentum conservation for *particles*, Compton could account for his observation

¹The magnitude k of the wave vector is related to the wavelength λ by $k = 2\pi/\lambda$, and its direction $\mathbf{k}/k = \hat{\mathbf{k}}$ is normal to the wavefront. We usually use the reduced wave length $\lambda = \lambda/2\pi$; also $\hat{\mathbf{a}}$ always stands for a unit vector.

that the scattered γ -rays had a wavelength λ' longer than that of the incident ray,

$$\lambda' = \lambda + 2\lambda_C \sin^2 \frac{1}{2}\theta \quad (2)$$

where

$$\lambda_C = h/mc \quad (3)$$

is the electron's Compton wavelength, 3.86×10^{-11} cm, and θ the laboratory scattering angle. Furthermore, Bothe and Geiger confirmed that the scattered electrons came off in coincidence at an angle correlated with that of the scattered photon as expected from these conservation laws.

From the classical perspective, the relations in Eq. 1 are a scandalous liaison between unrelated concepts — that of particle and wave. This is but one example of Bohr's *complementarity principle*, which asserts that to attain an understanding of phenomena in the quantum realm it is necessary to engage two or more concepts that are mutually inconsistent from the classical viewpoint. In Eq. 1 the complementary concepts constitute *wave-particle duality*. As we shall learn in chapter 10, when electrodynamics is reformulated as a quantum theory, this rather vague formulation of complementarity becomes much sharper: the γ -rays produced by Compton's radioactive source are states of the electromagnetic field with a definite number of photons, but in such states the field strengths do not have definite values. The states produced by an ideal laser, on the other hand, have well-defined field strengths, but not a definite number of photons. Here the complementary concepts are those of photon and field strengths; one or the other can be given a sharp meaning, but not both simultaneously.

In the Compton effect, the relation between wavelength and scattering angle is correctly given by (2), and the conservation of energy and momentum gives the observed angle at which the electron emerges once the photon's angle θ is specified, but that does not say *which* value of θ will be observed when the next radioactive decay produces a γ -ray. It is difficult, at best, to imagine anything the experimenter could do to specify further the collision in the hope of getting an in-principle prediction of the value of θ , e.g., by measuring the impact parameter between the photon and the electron, as one can do in a collision between billiard balls. This suggests that the only *empirically reproducible* data the experimenter can hope to find is the *probability distribution* for the scattering angle θ . Einstein's original "naive" photon concept has no means for calculating such a probability distribution. This can, it turns out, be done successfully with quantum electrodynamics.

The Compton effect also serves as an illustration of the correspondence principle. For incident light of low enough frequency or long enough wavelength, the scattered light has the same frequency and wavelength as the incident light. According to (2), here "long enough" means wavelengths long compared to the Compton wavelength, $\lambda \gg (\hbar/mc)$. When this inequality is satisfied, the angular distribution calculated from quantum electrodynamics reduces to the classical Thomson cross section.

A large body of evidence attesting to the wave nature of light had been accumulated in the century preceding the discovery of the photoelectric and Compton effects. How can the phenomena of interference and diffraction be reconciled with these corpuscular manifestations of light?

To examine this question, consider the diffraction of a plane wave incident normally on a transmission grating of parallel slits, each of width d , separated by D , with $D \gg d$. According to classical optics, the angular separation $\Delta\alpha$ between the

maxima in the interference pattern, and the angular width $\delta\alpha$ of each maximum, are

$$\Delta\alpha \approx (\lambda/D), \quad \delta\alpha \approx (d/D)\Delta\alpha \ll \Delta\alpha, \quad (4)$$

where λ is the wavelength. As detector of the transmitted light a photographic emulsion will do. If the light intensity is very low, and the plate is exposed for a sufficiently short time, a few dark spots will be seen, each due to a photochemical reaction triggered by a single photon. As the length of exposure is increased, the number of spots will increase and they will acquire a density distribution that approaches that of the classically predicted interference pattern. In short, the wave picture gives the correct probability for where a photon is detected.

If we accept the proposition that photons have corpuscular properties, this would presumably imply that the "size" of a photon is microscopic and small compared to a single slit. Then it is only natural to ask what would be observed if the plane wave that covers the whole grating were replaced by sequential exposures that illuminate just one slit at a time. According to classical optics, however, this would produce a succession of diffraction patterns from individual slit, which have an angular width λ/d , i.e., cover many of the maxima in the diffraction pattern when the whole grating is illuminated.

This consideration, and others of a similar vein, lead to an important conclusion:

In any setup that allows light to traverse different paths, these paths can either be combined coherently to form an interference pattern in which case the experiment cannot reveal which path a photon follows, or the apparatus can be modified to determine which path is followed but this destroys the interference pattern.

This is yet another illustration of complementarity: an arrangement designed to manifest one of the properties of a phenomenon expected from the classical viewpoint contains the possibility of observing at least some of the other classical properties. In this instance, the complementary properties are the wave property of interference and the particle property of path.

The elegant experiment sketched in Fig. 1.1 further elucidates the complementarity of the concepts of path and interference. Here two trapped and effectively stationary Hg^+ ions are illuminated by a laser beam. The photons that comprise this beam are scattered by the ions and then detected. Because the probability of scattering is small, the experiment is in effect a succession of individual photon collisions by one or the other of the two ions. If, for a moment, we assume the ions to be structureless, and that there is no such thing as polarization, the scattered light would have the same angular distribution as in the classical Young two hole interference experiment. The ions are, however, spin $\frac{1}{2}$ objects. Furthermore, the laser produces linearly polarized light, and the experiment can select scattered photons of various linear polarizations. As a consequence, by judicious choices of the polarizations of the incident and scattered photons, the events can be separated into two categories:

1. those in which there is *no possibility* that either ion underwent a spin flip ;
2. those in which one of the ions *must* have undergone a spin flip.

In case 1, it is impossible to determine which of the two ions was responsible for scattering, so the path taken by the photon is unknown in principle. In case 2, on the

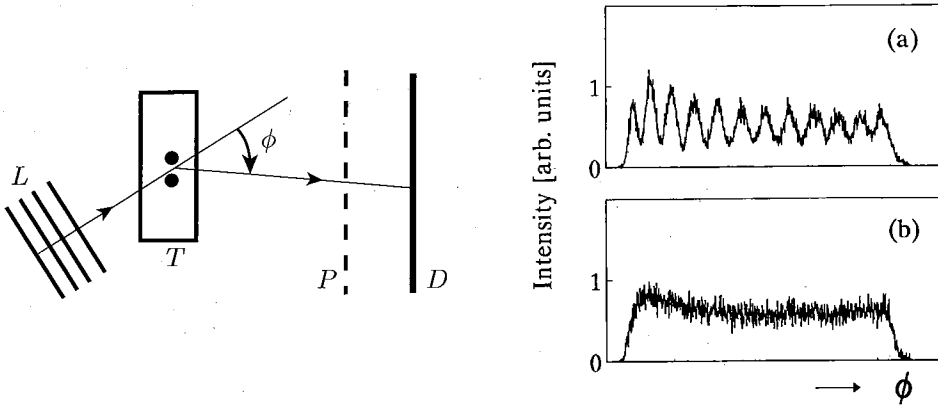


FIG. 1.1. Sketch of an interference experiment. L is a linearly polarized laser beam, T a trap that holds two Hg^+ ions effectively at rest, P a polarizer, and D a detections screen. (a) Events in which spin flip is excluded and the two possible photon paths are indistinguishable. (b) Events in which one of the ions must have had a spin flip which, in principle, determines the photon path. From U. Eichmann, J.C. Berquist, J.J. Bollinger, J.M. Gilligan, W.M. Itano, D.J. Wineland and M.G. Raizen, *Phys. Rev. Lett.* **70**, 2359 (1993). See also W.M. Itano et al., *Phys. Rev. A* **57**, 4176 (1998).

other hand, an examination of the spins of the ions after the photon has scattered would select which one caused the scattering and thus determine the photon's path. Hence the events in category 1 should show the Young interference pattern, while those in category 2 should not. The data confirming this is shown in Fig. 1.1.

Note well that in this experiment there is no instrument that actually measures the spin of the ions after scattering. This fact establishes two important points:

- The question of whether there is interference is settled solely by whether it is impossible or possible to determine which path is taken by a photon. Whether or not the determination is actually made does not matter.
- The “destruction” of the interference pattern arising from collisions where one ion has undergone a spin flip cannot be ascribed to some “irreducible disturbance caused by measurements” carried out on these photons. The collisions which do not cause a spin flip, and do produce the interference pattern, disturb the photons as much or as little as those in which there is a spin flip. To repeat the preceding point, all that counts is whether or not evidence exists that can reveal the photon's path.

For clarity's sake, the absence or presence of interference was just stated as a crystal clear distinction. The full story is that the visibility of the interference pattern diminishes as the confidence grows with which the photon path becomes knowable. For this purpose, consider diffraction by two holes in an opaque screen, with one of the holes being partially absorbing.¹ The amplitude and intensity are then

$$\varphi = ae^{ikL_1} + be^{ikL_2}, \quad |\varphi|^2 = a^2 + b^2 + 2ab \cos[(d/L)kx], \quad (5)$$

¹D.M. Greenberger and A. YaSin, *Phys. Lett. A* **128**, 391 (1988).

where $L_{1,2}$ are the distances from the two holes to the observation point, d is the separation of the holes, and L the separation between the screen to the parallel detection plane (assuming $d/L \ll 1$). If there is no absorber, a equals b . The visibility of the diffraction pattern can be defined as

$$V = \frac{|\varphi|_{\max}^2 - |\varphi|_{\min}^2}{|\varphi|_{\max}^2 + |\varphi|_{\min}^2} = \frac{2ab}{a^2 + b^2} \quad (6)$$

If two detectors are placed just behind the holes, they will register with rates proportional to a^2 and b^2 . The probabilities that any one photon takes one or the other path are then a^2/N and b^2/N , with $N = a^2 + b^2$, and their difference is

$$\Delta = \frac{a^2 - b^2}{a^2 + b^2} \quad (7)$$

Thus there is a smooth transition as $|a/b|$ departs from $a = b$, when the two paths are equally likely ($\Delta = 0$) and the visibility has its maximum value of $V = 1$, to zero visibility as $|b/a| \rightarrow 0$ when it is certain that every photon takes one of the two paths, i.e., $|\Delta| = 1$. Moreover,

$$V^2 + \Delta^2 = 1, \quad (8)$$

so there is a relationship between the degrees to which the complementary wave-like and particle-like features can be in evidence simultaneously. As V is linear in b , a substantial diffraction pattern survives even when $b^2 \ll a^2$ and it is reasonably safe to bet on the path of the next photon.

A similar conclusion applies to the famous debate in which Einstein proposed to determine which of two slits in a plate each particle traverses in contributing to a diffraction pattern by measuring the recoil of the plate, which Bohr showed is incorrect because the uncertainty principle must also be applied to the plate (see the discussion following Eq. 17). A more elaborate analysis shows that when measurement of the plate's recoil provides incomplete knowledge of which slit is traversed there is also a visible diffraction pattern.¹

(b) The Uncertainty Principle

The uncertainty principle emerges when the Einstein relations for the photon's momentum and energy are combined with the assumptions that the energy density of classical electrodynamics gives the probability of detecting individual photons in a given space-time volume. The classical electric field $\mathbf{E}(\mathbf{r}, t)$ in empty space satisfies

$$\left(\nabla^2 - \frac{1}{c^2} \frac{\partial^2}{\partial t^2} \right) \mathbf{E} = 0, \quad \nabla \cdot \mathbf{E} = 0, \quad (9)$$

with boundary conditions appropriate to the apparatus in question; so does the magnetic field. The most general solution of (9) is

$$\mathbf{E}(\mathbf{r}, t) = \int d\mathbf{k} e^{i(\mathbf{k} \cdot \mathbf{r} - \omega t)} \mathbf{a}(\mathbf{k}), \quad (10)$$

¹W.K. Wothers and W.H. Zurek, *Phys. Rev. D* **19**, 473 (1979); WZ.

where $\omega = ck$ and $\mathbf{k} \cdot \mathbf{a} = 0$. If the photon is detected in some region with sides Δx_i ($i = 1, 2, 3$), then the electromagnetic energy and momentum densities are nonzero in that region, and fall off quickly outside it. This requires $\mathbf{E}(\mathbf{r}, t)$ to have the same character. The theory of Fourier integrals then tells us that the size of the region in \mathbf{k} -space in which the Fourier amplitude $\mathbf{a}(\mathbf{k})$ is substantial is related to the size of the spatial region by

$$\Delta x_i \Delta k_j \gtrsim \delta_{ij}. \quad (11)$$

Furthermore, the time Δt that the packet takes to pass any point is related to the dispersion in frequency by

$$\Delta \omega \Delta t \gtrsim 1. \quad (12)$$

The Einstein relations then recast these inequalities for classical wave packet propagation into inequalities involving dispersions in photon momentum and energy,¹

$$\Delta x_i \Delta p_j \gtrsim \hbar \delta_{ij}, \quad \Delta E \Delta t \gtrsim \hbar. \quad (13)$$

These are the *Heisenberg uncertainty relations*, first formulated by him for non-relativistic particles, not photons. However, *once the ability to determine any object's momentum and energy is restricted by the uncertainty relations, those of all other objects with which it can, in principle, interact must also satisfy such restriction*, for if they did not, those other objects could be used to “defeat” the uncertainty principle.

It must be emphasized that momentum conservation must be used to reach this last conclusion, and plays a central role in what follows. *That energy and momentum are conserved by any isolated systems on an event-by-event basis, and not just as an average over a large number of events, is, as we shall see, a consequence of the fundamental principles of quantum mechanics.* It is supported by an enormous body of evidence, beginning with the experiments on Compton scattering done before the invention of quantum mechanics, and most strikingly by experiments that observe the recoil of electrons, nuclei, nucleons and other particles when they emit, absorb or scatter neutrinos.

If the uncertainty relations also hold for massive particles, that would suggest that they too display wave-particle duality. This supposition is confirmed by diffraction experiments first done with electrons, then with neutrons, and more recently with atoms. An especially striking illustration of the universality of wave-particle duality is given in Fig. 1.2, which shows the diffraction pattern of electrons scattered from a standing light wave. These all demonstrate that a *de Broglie wavelength*

$$\lambda_{\text{dB}} = \hbar/p \quad (14)$$

is to be ascribed to a particle of momentum p . Here, again, our tale is anachronistic, because de Broglie's conjecture was the opening breakthrough in the invention of quantum mechanics.

The uncertainty relations are still another manifestation of complementarity, for they stipulate that in a description of a system using one classical attribute, say,

¹The momentum-coordinate uncertainty relation is an unambiguous inequality that follows from the formalism of quantum mechanics, whereas the energy-time relation is more qualitative and subtle, a distinction that this argument fails to reveal. This issue will be discussed in §2.4(d).

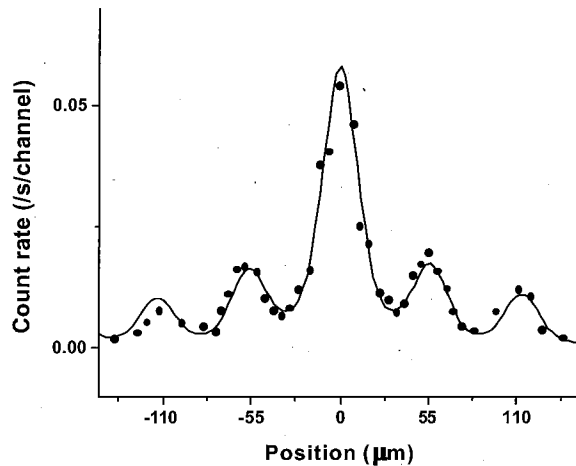


FIG. 1.2. Diffraction pattern produced by scattering electrons from the standing light wave created by two opposed lasers. From D.L. Freimund, K. Aflatooni and H. Batelaan, reprinted by permission from *Nature* **413**, 142 (2001) ©Macmillan Magazines, Ltd. The solid curve is based on the original theory by P.L. Kapitza and P.A.M. Dirac (*Proc. Camb. Phil. Soc.* **29**, 297 (1933)).

position, one surrenders the possibility of specifying the complementary classical attribute, momentum.

It so happens that Heisenberg derived the uncertainty relations by also using the Compton effect, but in the complementary sense — by analyzing to what extent the position and momentum of an electron can be determined. For this purpose he devised a famous thought experiment, the γ -ray microscope. His argument will not be repeated here. But one implication of the argument, recognized afterward by Pauli, is important and often overlooked.

The uncertainty relations do not say whether it is possible to determine one member of the pair x_i and p_i to arbitrary accuracy by surrendering all knowledge of the other. To increase the resolving power of the microscope, the wavelength λ of the scattered light that is to form an image of the electron must be shortened. But according to (2), the shortest wavelength attainable is of order the Compton wavelength \hbar/mc , unless the scattering angle θ approaches zero, in which circumstance the microscope would be swamped by the incident light. Furthermore, the wavelength varies across the microscope's aperture by an amount of order \hbar/mc , and this again limits the resolution to that same degree. The conclusion, therefore, is that a massive particle's position can only be determined to an accuracy of order its Compton wavelength λ_C ; no matter how poorly its momentum is known. From today's perspective this is not surprising, because for incident photon frequencies above $2mc^2/\hbar$, or wavelengths short compared to λ_C , pair creation becomes possible, and the notion that a measurement is being performed on a one-particle system breaks down. This remark is our first indication that the concepts of non-relativistic quantum mechanics must undergo far-reaching modifications when relativistic effects become important.

This conclusion does not mean that a massive particle's position can never be specified in quantum mechanics. The Compton wavelength is very short compared

to all lengths that characterize non-relativistic quantum states because λ_C vanishes in the nonrelativistic limit $c \rightarrow \infty$. Put in a dimensionless manner, the ratio of the Compton to de Broglie wavelengths is

$$\frac{\lambda_C}{\lambda_{\text{deB}}} = \frac{p}{mc} = \frac{v}{c}, \quad (15)$$

and therefore the inability to specify a massive particle's position to arbitrary accuracy is acceptable in nonrelativistic quantum mechanics.

By the same token, however, position is an ill-defined concept for the massless photon. A photon's position cannot be specified to better than the mean wavelength of the wave packet that describes its propagation. This distinction is reflected in the formalism. In nonrelativistic quantum mechanics, it is possible to define a probability distribution in coordinate space, and in momentum space.¹ In contrast, quantum electrodynamics allows an unambiguous definition of the momentum distribution for photons, but not of a photon probability distribution in coordinate space.

Several questions remain unsettled about the degree to which coordinates or momenta of massive particles can be determined.

First, can a definite time be assigned to a position determination? The uncertainty in time is the interval δt taken by the scattered photon of wavelength λ' to pass a point, which is given by

$$\delta t \approx \lambda'/c \gtrsim \hbar/mc^2. \quad (16)$$

This is the time required for light to traverse a Compton wavelength, and is negligible in nonrelativistic physics.

Second, is a position determination reproducible? After a time τ the particle struck by the γ -ray will have moved a distance $\tau(\mathbf{p} + \Delta\mathbf{p})/m$, and this stochastic drift can be reduced to any desired degree by repeating the measurement quickly enough. So, in the nonrelativistic regime, position determinations are, in effect, arbitrarily accurate and reproducible.

Third, can momenta be determined to arbitrary accuracy? To determine the momentum, a particle's position is measured at two points \mathbf{r}_1 and \mathbf{r}_2 with inaccuracies $\Delta\mathbf{r}_1$ and $\Delta\mathbf{r}_2$ sufficiently large to produce negligible uncertainty of the momentum, but small compared to the separation $L = |\mathbf{r}_1 - \mathbf{r}_2|$. By increasing L the accuracy can be refined to any desired degree, in contrast with the case of position determinations. The setup produces states that continue to have a well-defined momentum, because an almost free particle has a nearly constant momentum. On the other hand, a free particle state that has been determined to have a well-defined position has a large uncertainty in momentum, and as a consequence will lose its localization in a time that shrinks as the accuracy of the position determination increases.

Fourth, how quickly can a momentum determination be made? The preceding determination only produces a state of well-defined momentum after the long time interval Lm/p . But it can be used to prepare a target of low momentum particles for subsequent Compton scattering, and then a selection of the appropriate scattered photon will prepare a particle with the desired momentum. Because there is no need to form an image with the scattered photons in this case, the wavelength can be chosen so as to make the preparation time $\delta t \approx \lambda/c$ arbitrarily short.

¹Because of the uncertainty principle, it is not possible, however, to define a joint probability distribution in coordinates and momenta (i.e., in phase space). In this connection, see §2.2(f).

These considerations justify the assumption of nonrelativistic quantum mechanics that coordinate and momentum space probability distributions exist at a definite instant. It should be understood, however, that knowledge of the momentum distribution does not determine the coordinate distribution, or vice versa, for that would fly in the face of the uncertainty principle. To determine these distributions one must know the Schrödinger wave function, in either coordinate or momentum space; the wave function, however, cannot be computed from either or even both probability distributions except in very special cases.

Finally, we must still confirm that the uncertainty principle is a universal constraint, as it was assumed to be in extending it to massive particles from its first appearance for photons in our account.

Consider, first, a simple position measurement, in which a particle moving along the z -direction is passed through a perpendicular slit of width d , which determines the x -coordinate to within an uncertainty $\Delta x = d$. Diffraction will cause the beam to spread by an angle

$$\sin \theta \simeq \frac{\lambda}{d} \simeq \frac{\hbar}{p_z d}, \quad (17)$$

which produces an uncertainty Δp_x of momentum in the x -direction of order $p_z \sin \theta$. This conforms with the uncertainty principle, i.e., $d\Delta p_x \sim \hbar$. But the assumption that momentum conservation is strictly valid would imply that the uncertainty principle could be “defeated” if the screen’s momentum were precisely known. The latter precision is limited, however, by the requirement that the slit’s position must be known with a precision much better than d if the previous claim about the determination of the particle’s position is to stand, which implies that the screen has a momentum uncertainty much greater than \hbar/d . This greatly exceeds the uncertainty Δp_x of the particle’s momentum along x , which is of order \hbar/d , and therefore precludes a circumvention of the uncertainty principle. In a nutshell, consistency demands that the apparatus also obeys the uncertainty principle. (The screen’s mass is macroscopic, so its momentum uncertainty will produce negligible motion, and not undermine the position measurement.)

And now we can close the circle, so to say, by asking whether there are any restrictions on the accuracy of electromagnetic quantities beyond those on photon position and momentum, from which we began. There must be such restrictions because, if classical electrodynamics were left untouched, the position and momentum of a charged particle could be determined from the electric and magnetic field emanating from that particle. If those fields could be determined simultaneously with arbitrary precision, that knowledge could, once again, be used to “defeat” the uncertainty principle. Hence the uncertainty relations for the sources of the fields must also impose uncertainty relations on the fields.

The argument that leads to these relations, due to Bohr and Rosenfeld, is subtle and will be sketched in §10.2 after the quantum theory of the electromagnetic field has been developed. In brief, they noted that field strengths cannot be measured at mathematically sharp space-time points, but must be done with test charges of finite spatial extent V whose response to the fields is observed over a finite time interval T , because the response of point test bodies would be infinitely large as they would be sensitive to arbitrarily high frequency modes of the field. Hence, realistic measurements determine an average over the space-time volume $\Omega = VT$ of, say, the electric field, $\bar{E}(\Omega)$, where Ω can be as small as one pleases, but must be finite.

The uncertainty in momentum and position of a charged test body will cause it to radiate uncertain electromagnetic fields which will confuse field measurements by another test body in another space-time region, and thereby produce an uncertainty in the fields in the latter region.

One example of such a field uncertainty relation is that for uncertainties in space-time averaged electric field components:

$$\Delta \bar{E}_x(\Omega_1) \Delta \bar{E}_y(\Omega_2) \geq \left| \frac{\hbar}{8\pi\Omega_1\Omega_2} \int_{\Omega_1} d\Omega_1 \int_{\Omega_2} d\Omega_2 \frac{\partial^2}{\partial x_1 \partial y_2} \frac{\delta(t - r/c)}{r} \right|. \quad (18)$$

The integral runs only over the portions of the two regions, Ω_1 and Ω_2 , that can be connected by light signals, because the delta-function vanishes unless the distance r and time difference t between the two space-time integration points constitute a light-like interval.

This elegant result has two features that should be noted. First, the uncertainty product does not depend on the charge or mass of the test bodies, but depends only on the natural constants and on the regions in which the fields are measured, and of course it vanishes as $\hbar \rightarrow 0$. Thus this is an important illustration of the universality of the uncertainty principle. Second, if the two regions cannot be connected by light signals, then there is no restriction on the accuracy to which the two fields in question can be determined, because no measurement in one region can then produce an effect in the other region. This is an example of the relativistic causality principle, which plays a central role in quantum field theory.

A last, important, word. Precisely the same result, Eq. 18, will be derived in §10.2 from the "canonical" quantum theory of the electromagnetic field without resort to intuitive arguments involving test bodies, or order-of-magnitude estimates. Such concordance between heuristic and formal arguments should always be demanded of a basic theory.

1.2 Superposition

Quantum mechanics is a strictly linear theory, and all experimental data are consistent with this assumption. In the history of physics, it is the first and only basic theory with this property. Newton's equations are linear only in special circumstances, such as harmonic motion. Maxwell's equations are linear in empty space, but lose that property when charges are present. The theory of gravitation, general relativity, is inherently nonlinear. All this does not mean that quantum mechanics does not lead to nonlinear effects. Obviously it must, or it could not even reduce to classical mechanics and electrodynamics in the appropriate limit. So what does the opening sentence then mean?

(a) *The Superposition Principle*

The Schrödinger equation, for any system no matter how complicated, has the form

$$\left(H - i\hbar \frac{\partial}{\partial t} \right) \Psi(t) = 0, \quad (19)$$

where H is the Hamiltonian and $\Psi(t)$ the wave function. The specifics of the system, including such essentials as the number and types of degrees of freedom it possesses,

and whether it is to be treated in a Lorentz-invariant manner by quantum field theory, are buried in the form of H , which will then be reflected in Ψ . But all such “details” have no bearing on the following fact: if $\Psi_1(t)$ and $\Psi_2(t)$ are any two solutions of (19), and $c_{1,2}$ are arbitrary complex numbers, then the linear superposition

$$\Psi(t) = c_1\Psi_1(t) + c_2\Psi_2(t) \quad (20)$$

is also a solution of the Schrödinger equation (19).

This fundamental statement is called the *superposition principle*. In important respects it is the most profound principle of quantum mechanics, and it is often the root cause of those features of quantum mechanics that are most enigmatic from the perspective of our everyday experience. In this section we examine some of the surprising implications of the superposition principle.

The discussion of the preceding section already exploited superposition repeatedly — for example, in connection with the diffraction grating, and in other situations where electromagnetic or de Broglie waves were superposed coherently. These are all examples that have a more or less direct counterpart to phenomena in classical optics. The full import of the superposition principle can only be appreciated, however, by considering phenomena that have no classical counterpart.

The simplest examples of these deeply non-classical features are provided by two-particle states. This was first revealed by Heisenberg’s treatment of the helium spectrum in 1926, in which, among other things, he showed that what would appear to be a magnetic interaction between electrons is really due to two-particle interference; this topic will be taken up in §6.2. A fuller appreciation of the astonishing properties of many-particle states, and their implications for the foundations of quantum mechanics, arose from a 1935 paper by Einstein, Podolsky and Rosen, cited henceforth as EPR. This paper and related topics are treated at length in chapter 12.

(b) Two-Particle States

All the examples considered in §1.1 involved superposition of waves in three-dimensional coordinate space, as in classical optics or in acoustics. The Schrödinger equation deals with waves in a three-dimensional space only in the special instance of one-particle systems, however, in which case $|\Psi(\mathbf{r}, t)|^2 d^3r$ is the probability for finding one particle in an infinitesimal interval about the point \mathbf{r} in everyday space. But if quantum mechanics is to supercede classical mechanics, it must, for an N -body system, specify probability distributions in $3N$ coordinates; that is, it must deal with waves not in three-dimensional coordinate space but in $3N$ -dimensional configuration space. This is evident in the simplest situation, a system of N free particles of mass m , in which case the Schrödinger equation is

$$-\frac{\hbar^2}{2m}\nabla_N^2\Psi(\mathbf{r}_1\ldots\mathbf{r}_N;t) = i\hbar\frac{\partial}{\partial t}\Psi(\mathbf{r}_1\ldots\mathbf{r}_N;t), \quad (21)$$

where ∇_N^2 is the Laplacian in $3N$ dimensions,

$$\nabla_N^2 \equiv \sum_{i=1}^N \left(\frac{\partial^2}{\partial x_i^2} + \frac{\partial^2}{\partial y_i^2} + \frac{\partial^2}{\partial z_i^2} \right). \quad (22)$$

The multi-dimensional wavelike character of quantum states, which has no counterpart in classical wave phenomena, gives the concept of coherence a more subtle and richer meaning in quantum mechanics than it has in classical optics, and leads to phenomena that are astonishing and counterintuitive from a classical perspective.

It suffices for now to consider two-body systems without mutual interactions, the generalization to $N > 2$ being rather straightforward. The Hamiltonian is then

$$H = H_1 + H_2, \quad (23)$$

where H_i is the Hamiltonian of body i . Each body (e.g., a many electron atom) may have internal degrees of freedom which interact with each other. All that matters is that there be no interaction between the two bodies. Two distinct types of Schrödinger equations then come into play. The complete two-body equation

$$(H_1 + H_2)\Psi(q_1 q_2; t) = i\hbar \frac{\partial}{\partial t} \Psi(q_1 q_2; t), \quad (24)$$

and the one-body equations

$$H_i \psi_{a_i}(q_i; t) = i\hbar \frac{\partial}{\partial t} \psi_{a_i}(q_i; t), \quad (25)$$

where q_i stands for *all* the coordinates of body i , including those needed to describe its internal motions, and a_i is a label that distinguishes between the different solutions of this last equation.

Because H_1 does not depend on the coordinates of particle 2, and vice versa, H acting on the product of one-body wave functions results in

$$(H_1 + H_2)\psi_{a_1}(q_1; t)\psi_{a_2}(q_2; t) = \psi_{a_2}(q_2; t)(H_1\psi_{a_1}(q_1; t)) + \psi_{a_1}(q_1; t)(H_2\psi_{a_2}(q_2; t)),$$

and therefore

$$\left(H - i\hbar \frac{\partial}{\partial t}\right) \psi_{a_1}(q_1; t)\psi_{a_2}(q_2; t) = 0. \quad (26)$$

Hence a product of one-body wave functions, $\psi_{a_1}(q_1; t)\psi_{a_2}(q_2; t)$, is a solution of the two-body Schrödinger equation provided there is no interaction between them.¹ As the two-body equation (24) is linear, the superposition of such products,

$$\Psi(q_1 q_2; t) = \sum_{a_1 a_2} c_{a_1 a_2} \psi_{a_1}(q_1; t)\psi_{a_2}(q_2; t), \quad (27)$$

where the $c_{a_1 a_2}$ are arbitrary complex constants, is again a solution of the Schrödinger equation for a non-interacting two-body system. It is essential to note that in the preceding sentence "constants" means just that — *independent of time*.

If there is an interaction, the Hamiltonian will have an additional term involving the coordinates of both particles, $H_{12}(q_1 q_2)$, and a product of one-body wave

¹In the language of partial differential equations, this is just the method of separation of variables. Put in the more abstract form used here, it is not only more transparent, but it is illustrative of quantum mechanical thinking. That is, if A_1 and A_2 are any two operators that commute with each other (as do H_1 and H_2 because they act on different variables), then eigenstates of $A_1 + A_2$ are products of separate eigenstates of A_1 and A_2 . Those who find this illuminating comment inscrutable should ignore it for now; it will be explained in detail in §2.1.

functions is then no longer a solution, nor are linear combinations with constant coefficients. For now we are only concerned with interactions of finite range, however, in which case the simple solutions (27) remain valid in many circumstances. That is, if the coordinates q_i are separated into a center-of-mass position \mathbf{r}_i , and internal coordinates, then in such systems H_{12} tends rapidly to zero as the separation $R = |\mathbf{r}_1 - \mathbf{r}_2|$ becomes large compared to an appropriate microscopic length scale, e.g., the Bohr radius $\sim 10^{-8}$ cm if the bodies are neutral atoms. At such separations, therefore, $H = H_1 + H_2$, and Eq. 27 is a solution wherever R is large compared to that scale. Furthermore, if the bodies are not involved in any processes sufficiently energetic to excite their internal motions, then in such an energy regime they are in effect “elementary” particles, and their wave functions can be treated as if they depend only on the center-of-mass coordinates \mathbf{r}_i . We will, therefore, often use the terms *particle*, *system* and *body* indiscriminately.

(c) Two-Particle Interferometry

Two-particle states can display interference effects if both particles are detected in coincidence while not showing conventional one-particle interference patterns. This is the phenomenon we shall now examine with the help of a simple and yet quite realistic *Gedanken* (or thought) experiment. Careful study of this experiment proves to be a sound investment for it reveals features that are central to both the formulation and interpretation of quantum mechanics.

Consider two particles a and b described by a wave function $\Psi(\mathbf{r}_a \mathbf{r}_b; t)$. From Ψ we can form the joint probability distribution

$$P_{ab}(\mathbf{r}_a \mathbf{r}_b; t) = |\Psi(\mathbf{r}_a \mathbf{r}_b; t)|^2. \quad (28)$$

This is the probability of detecting a at \mathbf{r}_a and b at \mathbf{r}_b in coincidence. We can also form the one-particle probability distributions, e.g., that for detecting a when b is not observed at all:

$$P_a(\mathbf{r}_a; t) = \int d^3 r_b P_{ab}(\mathbf{r}_a \mathbf{r}_b; t). \quad (29)$$

Our purpose is to establish the following assertion:

In any experimental setup that allows the two particles to traverse different paths, and in which *it is possible, in principle, to determine the path taken by one particle by some observation on the other*, neither particle will, by itself, display an interference pattern (i.e., in P_a or in P_b), but there may be an interference pattern in the a - b coincidence rate P_{ab} , i.e., in the correlation of positions for a and b . On the other hand, if the setup is such that *no observation on one particle can, in principle, determine the path of the other*, then either particle by itself, or both, may display an interference pattern (i.e., in P_a and/or P_b).

The words “in principle” are critical here. They allude, as we shall see, to the fact that *whether an observation is or is not made does not matter — what matters is whether such an observation is possible at all*.¹

¹Note also the similarity to the statement on p. 4 regarding one-particle interference effects.

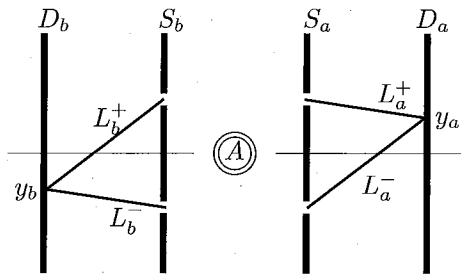


FIG. 1.3. Two-particle interferometer. The free particle A undergoes the two-body decay $A \rightarrow a + b$, with a passing through one of the two pin holes on the right and then detected on the right-hand screen, while b does the same on the left.

The state that will be analyzed to establish these contentions describes the particles produced in a decay process $A \rightarrow a + b$, and the experimental setup is the two-particle interferometer shown in Fig. 1.3. This consists of two parallel opaque screens S_a and S_b , each pierced by two pinholes symmetrically placed about the axis normal to the screens, and two parallel detection screens D_a and D_b sensitive only to a and b , respectively. The detectors record the coordinates of particles striking them in coincidence, i.e., determine the joint probability distribution P_{ab} of Eq. 28. This thought experiment is not far-fetched because there are several real-life examples of A . One is positronium, the bound electron-positron system, whose ground state annihilates into two photons; another is the neutral kaon K^0 , a particle that decays into two π mesons.

In the process $A \rightarrow a + b$ momentum is conserved, and so the decay products (daughters) will go in exactly opposite directions if A was at rest. Then if a passes through one of the two holes on the right, b must pass through the diametrically opposed hole on the left, and therefore a determination of the path of one determines that of the other. On the other hand, if A were at rest its position would be totally uncertain; it could be anywhere with respect to the interferometer. Conversely, if A is at the exact center of the setup, its momentum would be totally uncertain, there would be no correlation between the directions of a and b , and observation on one daughter would not determine the path of the other.

Hence A 's vertical localization s must exceed some lower limit to assure that the daughters can only pass through one pair of diametrically opposed pinholes. This limit is set by the uncertainty principle and momentum conservation. The former states that A 's momentum uncertainty satisfies $\Delta p_A \gtrsim \hbar/s$; the latter that the spread in angles Θ between the daughters' momenta (see Fig. 1.4(b)) is given by $\Theta \simeq (\Delta p_A / \hbar k) \gtrsim (1/sk)$, where we assume that the energy release in the decay is large enough so that both daughters have momenta of approximately the same magnitude $\hbar k$. But if the source A is to only illuminate one or the other of the opposed holes, Θ must be much smaller than ϕ , the angle subtended by the two pinholes on one screen as seen from A . Consequently, the condition on A 's localization is

$$s \gg \frac{1}{k\phi}. \quad (30)$$

We now turn to the daughters' wave function $\Psi_{\text{out}}(\mathbf{r}_a \mathbf{r}_b)$ outside the screens S_a and S_b . In this region they do not interact with each other, and therefore Ψ_{out} must

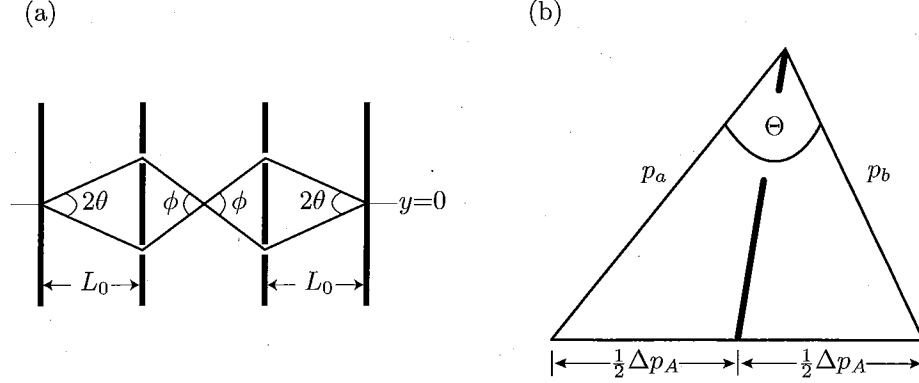


FIG. 1.4. (a) Angles pertaining to the two-particle interferometer. (b) Kinematics in the process $A \rightarrow a + b$.

be a linear combination of products of one-particle wave functions of the form (27), with each particle's wave function being a spherical wave $\psi(r) = e^{ikr}/r$ emanating from one of the pinholes. For example, one such term is $\psi(L_a^+)\psi(L_b^-)$, for the case where a emerges from the upper hole on the right and b from the lower one on the left, with the distances $L_{a,b}^\pm$ being defined in Fig. 1.3.

In general, Ψ_{out} is a linear combination of four such products with four arbitrary coefficients determined by matching $\Psi_{\text{out}}(\mathbf{r}_a \mathbf{r}_b)$ to the interior wave function $\Psi_{\text{in}}(\mathbf{r}_a \mathbf{r}_b)$ at the pinholes. Nothing essential is lost, and considerable simplification is gained, by considering the case where A is in a spherically symmetric wave packet. In this case the initial state A is invariant under reflection through the $y = 0$ plane perpendicular to the interferometer, which is equivalent to a rotation through π about an axis perpendicular to the interferometer's symmetry axis. Assuming that the interaction responsible for the process $A \rightarrow a + b$ is invariant under rotations, the daughters' state $\Psi_{\text{in}}(\mathbf{r}_a \mathbf{r}_b)$ must have the same reflection symmetry, and as a consequence the values of this wave function at the four pinholes are given by just two complex numbers:

$$\Psi_{\text{in}}(\mathbf{r}_a^+ \mathbf{r}_b^-) = \Psi_{\text{in}}(\mathbf{r}_a^- \mathbf{r}_b^+) = \alpha, \quad \Psi_{\text{in}}(\mathbf{r}_a^+ \mathbf{r}_b^+) = \Psi_{\text{in}}(\mathbf{r}_a^- \mathbf{r}_b^-) = \beta, \quad (31)$$

where $\mathbf{r}_{a,b}^\pm$ are the positions of the pinholes.

These coefficients have a simple meaning: $|\alpha|^2$ is the probability for a and b to pass through diametrically opposed holes, i.e., for A to have undergone back-to-back decay, whereas $|\beta|^2$ is the probability for both to pass through either the two upper or two lower holes. Clearly, $|\beta/\alpha|^2 \ll 1$ if the initial state of A satisfies the source size condition (Eq. 30).

The outside wave function evaluated at the detectors, when (31) holds, is

$$\Psi_{\text{out}} \doteq \alpha \left(e^{ikL_a^+} e^{ikL_b^-} + e^{ikL_a^-} e^{ikL_b^+} \right) + \beta \left(e^{ikL_a^+} e^{ikL_b^+} + e^{ikL_a^-} e^{ikL_b^-} \right). \quad (32)$$

Here the distance L_0 from the screens to the detectors is assumed to be much larger than that between the holes on either screen, so that the denominators in e^{ikr}/r can all be replaced by L_0 , which has been absorbed into an irrelevant overall factor, and \doteq means equal apart from such a factor. In this geometry (the Fraunhofer

diffraction limit), the various lengths can be approximated by

$$L_a^\pm \simeq X \mp \theta y_a, \quad L_b^\pm \simeq X \mp \theta y_b, \quad (33)$$

where X is the same length in all four cases, while θ and the y coordinates are defined in Fig. 1.4. With these small-angle approximations, (32) simplifies to

$$\Psi_{\text{out}}(y_a y_b) \doteq \alpha \cos[k\theta(y_a - y_b)] + \beta \cos[k\theta(y_a + y_b)]. \quad (34)$$

The novel two-particle interference phenomena require, as we will now see, that the decay be dominantly back-to-back, that is, $|\beta/\alpha|^2 \simeq 0$. The joint probability distribution for detecting a at y_a and b at y_b in coincidence is then

$$P_{ab}(y_a y_b) \doteq |\cos[k\theta(y_a - y_b)]|^2. \quad (35)$$

This asserts that *the coincidence rate will display an interference pattern in the variable $|y_a - y_b|$, the "distance," so to say, between locations on the widely separated detection screens.*

In striking contrast, *the distributions of locations of particles on the individual detection screens show no interference pattern.* This is so because, according to (29), the probability for detecting a at y_a regardless of where b struck the other detector, is

$$P_a(y_a) = \frac{1}{2Y} \int_{-Y}^Y dy_b P(y_a, y_b) = \text{const.} + O(1/Y). \quad (36)$$

This distribution is independent of a 's position, a result that requires the size $2Y$ of the detection region for b to be large enough to yield no information about b 's position, i.e., $Y \gg (1/k\theta)$, the distance between interference fringes.

Quantum optics experiments that confirm the remarkable effect just described have been done, though for technical reasons, not by using photon pairs produced in a momentum-conserving decay such as just discussed. The results of an outstanding example are shown in Fig. 1.5.

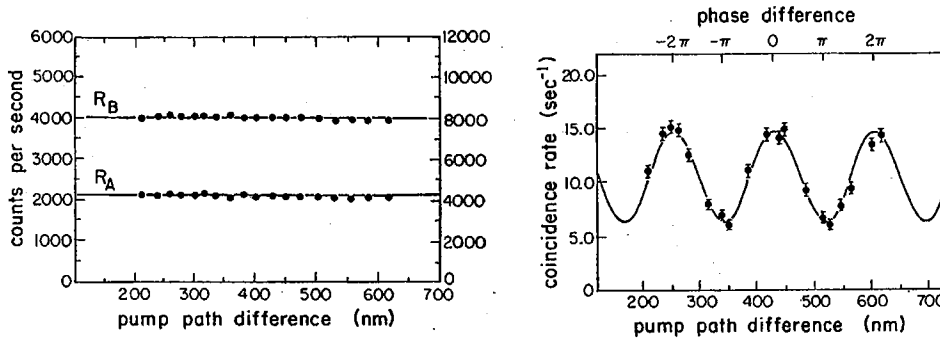


FIG. 1.5. Results of a two photon interference experiment which is effectively equivalent to the setup in Fig. 1.3 (L. Mandel, *Rev. Mod. Phys.* **71**, S274 (1999)). The horizontal scales are the counterpart of $y_a - y_b$. On the left are the singles rates at the two detectors D_a and D_b , on the right the coincidence rate, with the solid line being the theoretical expectation.

The existence of interference effect in the coincidence rate when there is none in the individual rates is a quantum mechanical phenomenon. Hence it is important to understand why this initially surprising result is, in retrospect, not surprising!

The absence of an interference pattern in the individual rates is due to the possibility of determining the path that both particles took by an observation on just one. To accomplish this one can, for example, replace b 's position detector D_b by a device that determines b 's momentum along y as it arrives at the left-hand detection plane. This would determine which hole in S_b it traversed, and because of the back-to-back decay which hole in the other screen was traversed by a . Hence there can be no interference pattern in the locations of a 's position, for that would require a coherent addition of amplitudes from the two holes on the right side, which is excluded by the knowledge of which hole a traversed. Of course, the same conclusion holds for b .

The preceding paragraph might lead one to suspect either an error or a swindle, because it talks of an apparatus that measures position *and* momentum of one and the same object, which is impossible if the uncertainty principle is valid. The suspicion is unfounded, however. The experimental setup measures momentum *or* position, with the choice of which measurement is actually made being on an event-by-event basis, and if one wishes decided only *after* the decay $A \rightarrow a+b$ has occurred while the daughters are still *en route*. It is this feature of two-particle states that lies at the heart of EPR experiments, which will be discussed shortly.

To shed further light on what has just been discussed, consider what happens if the back-to-back decay does not dominate, and β is not negligible. In particular, consider the case where the source size s is small enough so that the two holes on either side are illuminated equally, i.e., $\alpha = \beta$. Then (34) becomes

$$\Psi_{\text{out}}(y_a y_b) = \cos(k\theta y_a) \cdot \cos(k\theta y_b), \quad (37)$$

which describes *independent* diffraction patterns on each of the two detection screens. There are no correlations in either coordinates or momenta, the reason being that determining which hole was traversed by one particle does not determine which path the other took.

The interference pattern in the coincidence rate when back-to-back decay dominates is due to a correlation in the momenta of a and b . At the detecting planes the particles have y -components of momentum, p_a and p_b , that are either $\hbar k\theta$ or $-\hbar k\theta$. At each detector there is a random distribution of events with $\pm \hbar k\theta$, but a *strict correlation* between those on the right and left: if one particle has momentum $\hbar k\theta$, the other is *guaranteed* to have $-\hbar k\theta$. The formalism needed to relate this correlation in momenta to a correlation in positions will only be developed in the next chapter. Briefly put, the coordinate space wave function $\Psi_{\text{out}}(y_a y_b)$ is the Fourier transform of a wave function in momentum space $\Phi(p_a p_b)$, and the latter just expresses the earlier sentence in precise terms:

$$\Phi = \delta(p_a - \hbar k\theta) \delta(p_b + \hbar k\theta) + \delta(p_a + \hbar k\theta) \delta(p_b - \hbar k\theta), \quad (38)$$

where $\delta(p)$ is the Dirac delta function, which is the statement that the momentum is precisely p . When this expression is Fourier transformed, it immediately leads to $\cos[k\theta(y_a - y_b)]$, in agreement with (32) when $\beta = 0$.

(d) EPR Correlations

The phenomena revealed by the two-particle interferometer have remarkable features that Einstein called “spooky action-at-a-distance,” and which were first discussed by Einstein, Rosen and Podolsky (EPR).

There is, of course, nothing novel about using a particular measurement on one particle to determine a property of another that is, at the time, arbitrarily far away. If it is known that a missile with known linear and angular momenta will separate into two pieces, it suffices to determine these momenta of one piece to determine those of the other. Here, however, there are remarkable features that are totally foreign to classical physics. The wave-like correlation in position between particles that are arbitrarily far apart is such a feature — a feature that is complementary (in Bohr’s sense) to the sharp correlations in their momenta, Eq. 38. While this momentum correlation seems very natural from a classical perspective, it must not be forgotten that the observed momentum distribution $|\Phi(p_a p_b)|^2$ is a coherent superposition of the two classically understandable terms in (38).

It is even more remarkable that a *free choice* between determining the position or momentum of b assigns the distant particle a , *without disturbing it*, to distinct categories of events that form distinct diffraction patterns. Furthermore, this choice can be made while the particles are on the way to the detectors. This feature is not evident with arbitrarily small pinholes, because such an idealized aperture produces no angular variation in intensity. With a finite aperture of width $2d$, the one-particle distribution is no longer uniform, as it is Eq. 36, but becomes

$$P_a(y_a) \doteq \left| \frac{\sin k\epsilon(\rho - y_a)}{k\epsilon(\rho - y_a)} \right|^2 + \left| \frac{\sin k\epsilon(\rho + y_a)}{k\epsilon(\rho + y_a)} \right|^2, \quad (39)$$

where $\epsilon = d/L_0$, $\rho = l + \frac{1}{2}\varphi L_0$, and $2l$ is the distance between the pinholes. This is the incoherent sum of two conventional one-hole diffraction patterns with centers separated by 2ρ .

This EPR feature can be demonstrated by the following experiment. On the right, the apparatus always measures the coordinate of a ; and on the left, the apparatus switches at random between measurements of position or momentum of b . All measurements are done in coincidence. This does not require communication between the widely separated laboratories, because there can be a protocol to insert only one specimen of A at regularly spaced intervals sufficiently long to insure that both laboratories carry out observations on the same $a + b$ specimen. After the run is over, the list of choices that were made in observing b is transmitted to the distant laboratory, where the data on the coordinate of a are separated into three sets: (1) those where $p_b = \hbar k\theta$, (2) those where $p_b = -\hbar k\theta$, and (3) those where y_b was measured. No human intervention is necessary after the apparatus is set to work; the collection, transmission and processing of the data can be fully automated.

The predictions of quantum mechanics are that

- set (1) will display the diffraction pattern of the upper hole alone (the first term of Eq. 39);
- set (2), the diffraction pattern of the lower hole (the second term);
- set (3), the oscillating correlation function $|\cos[k\theta(y_a - y_b)]|^2$.

While this particular experiment has not been done, enough experiments of the EPR variety have been so that there is no reason to doubt that what has just been claimed would be confirmed.

This setup provides no means for instantaneous signaling between the left-hand and right-hand laboratories. The observations on a in themselves give no information about what is learned about b in coincidence. No correlation can be elicited until the list of observation by one arm of the experiment are combined with the data from the other arm.

The interference patterns displayed, or not displayed, by the two-particle wave function are, to underscore it yet again, determined by what the experimenter can in principle do, and not by what may actually be done. This is best brought out by the *delayed choice* property — by the freedom to decide whether the momentum or coordinate is to be determined just before the particles are actually detected. What counts is whether the option to make this choice exists, and not whether the option is exercised. If the wave function is to pass the delayed choice test, it must possess a sufficient richness of properties to cope with a measurement that will be done in the future. It must, in this example, be able to display itself in a wave-like or particle-like guise, or in various combinations of these guises, depending, so to say, on what question will be asked of it.

The two cases discussed in detail, the one where there are independent one-particle diffraction patterns and no interference effects in the coincidence rate, and the other where there is an interference effect in the coincidence rate but no one-particle diffraction patterns, are limiting cases of the general situation described by Eq. 32 for arbitrary values of β/α . The quality that changes along this continuum is the degree of confidence with which it is possible to determine the path of one particle by an observation on the other.¹ If $\beta = 0$, it is known for sure which path a took from a momentum measurement on b , but as β increases this becomes progressively less certain, and the two possible paths become equally probable when $\beta = \alpha$. The smooth transition from two-particle to one-particle interference goes hand-in-hand with this decrease of knowledge attainable *in principle*.

1.3 The Discovery of Quantum Mechanics

Quantum mechanics is among the great intellectual achievements of the 20th century, and how this came about is interesting in itself. The following only offers the briefest of sketches.

The history separates naturally into two eras: 1900–1925, the development of the “Old Quantum Theory”; and 1925 to circa 1935, in which quantum mechanics and electrodynamics were discovered and their principal features elucidated.

In 1900 Max Planck discovered that he could only account for the spectrum of thermal radiation, which was in violent contradiction with classical electrodynamics, by assuming that the material sources of radiation have a discrete (“quantized”) energy spectrum. That this entailed a grave contradiction with classical physics was

¹This complementarity between one-particle and two-particle interference, which is related to the confidence of knowledge about paths, can be phrased quantitatively as a relationship, similar to (8), between the visibility of the corresponding diffraction patterns; see G. Jaeger, A. Shimony and L. Vaidman, *Phys. Rev. A* **51**, 54 (1995).

clear to Planck and troubled him. In 1905, Albert Einstein produced a much deeper departure from classical concepts by applying quantization to the thermodynamics of the electromagnetic field itself, introduced what was later to be called the photon, and predicted correctly the basic feature of the photo-electric effect. Although this and later Einstein papers on the quantum theory had a great influence, his idea that light has corpuscular aspects was only widely accepted after the discovery of the Compton effect in 1923. The next major step came in 1913 with Niels Bohr's quantum theory of the hydrogen spectrum based on Ernest Rutherford's model of the atom. This led to a great advance in the understanding of atomic structure and spectra, as can be seen in the massive 1924 edition of Arnold Sommerfeld's *Atombau und Spektrallinien*. The culminating theoretical advances of this first period were Wolfgang Pauli's exclusion principle and the discovery of electron spin² by Samuel Goudsmit and George Uhlenbeck, both in 1925.

Experimental physics played an indispensable role throughout this first period, of course. The 19th-century studies of thermal ("black body") radiation gave the first clearcut demonstrations that classical physics suffers from fatal deficiencies. In 1914 the Franck-Hertz experiment used inelastic electron scattering to establish that atoms did indeed have quantized excitation energies; in 1921 the Stern-Gerlach experiment demonstrated the quantization of angular momentum; and to repeat, in 1923 Arthur Compton performed his fundamental experiment on the scattering of γ rays. These were, of course, only the highest peaks of an imposing mountain range that held many riches that were to prove invaluable in what was to come.

The practitioners of the Old Theory understood full well that a logical structure was lacking — that it was not really a theory, but a jumble of folklore and recipes with many striking successes and deep insights undermined by perplexing failures.¹

The discovery of quantum mechanics arose from two distinct and seemingly unrelated streams of ideas: wave mechanics and matrix mechanics. Wave mechanics started first in 1923–24 with Louis de Broglie's suggestion that massive particles have wave-like properties — that wave-particle duality does not only apply to photons. This idea did not take on a powerful form until Erwin Schrödinger discovered his wave equation in 1926. Before then matrix mechanics had been initiated by Werner Heisenberg in the summer of 1925 and was already well established by year's end.

Heisenberg sought to focus on what is actually observable and to discard notions, such as electronic orbits in atoms, which he argued are not. He therefore replaced the classical coordinates and momenta of a charged particle by arrays of observable radiative transition amplitudes. Then he showed that these arrays obey a noncommutative algebra whose rules were constrained by empirically confirmed knowledge about radiative transitions that had been developed with the Old Theory, such as the Kramers-Heisenberg dispersion formula (see §10.7). In keeping with Bohr's correspondence principle, which states that the quantum theory must reduce to classical theory in the limit of large quantum numbers, Heisenberg assumed that his arrays obeyed equations of motion that had the same form as those of classical

²Electron spin was also proposed at the same time by R. de L. Kronig, but not published because Pauli convinced him the idea was nonsensical. It is said that the Nobel Prize was never awarded for electron spin because of this.

¹In this connection, Hans Bethe recalled that he had a great advantage over older people in learning quantum mechanics in 1926 because he did not know the Old Quantum Theory!

mechanics. It should be said that this ground-breaking paper, which Heisenberg in private referred to as “fabricating quantum mechanics,” is very difficult to follow, in contrast to most of the others that will now be referred to.

That Heisenberg’s arrays are matrices was quickly recognized by Max Born, who with Pascual Jordan then derived the canonical (q, p) commutation rule. This was followed, in November 1925, by the Born, Jordan and Heisenberg *magnum opus* which gave a nearly complete formalism: conservation laws, angular momentum, canonical transformations, some stationary state perturbation theory, and a first stab at quantization of the electromagnetic field. Independently, and based only on Heisenberg’s first paper, Paul Dirac in the same month presented a development of almost comparable sweep that postulated a correspondence between classical Poisson brackets and commutation rules. Finally, in January 1926 Pauli published his *tour de force* matrix mechanics solution of the Kepler problem, including both the Stark and Zeeman effects (see §5.2 and §5.4(c)).

Schrödinger called his papers “Quantization as an Eigenvalue Problem.” His approach was inspired by de Broglie’s suggestion and the analogy between geometrical optics and classical point mechanics that William R. Hamilton had created in the 1830s. Schrödinger’s first paper, submitted in January 1926, put forward the time-independent wave equation. His point of departure was to replace Hamilton’s characteristic function W by $\hbar \log \psi$ in the Hamilton-Jacobi equation (see §2.8(a)). From this he formulated a variational principle which led to the wave equation, and he then showed that its eigenvalues in the case of a Coulomb field reproduce the Bohr spectrum. In the following half year Schrödinger published a series of papers which also produced the complete theory. Particularly noteworthy was his demonstration that his “wave mechanics” is mathematically equivalent to “matrix mechanics.”

Among the many successful early applications of quantum mechanics three merit special attention. First, in 1926, Heisenberg’s successfully analyzed the He spectrum, which had baffled the Old Theory. In solving this problem he discovered that the Pauli principle requires antisymmetrical wave functions¹ (something which he could only do with Schrödinger’s theory!), and that the correlations resulting therefrom produce large electrostatic level splittings that look as if they are magnetic in origin (see §6.2). Second, also in 1926, Born used Schrödinger’s equation to solve the first scattering problem, a phenomenon that the Old Theory could not even formulate, and in doing so introduced the interpretation of $|\psi(\mathbf{r})|^2$ as a probability distribution. And third, in 1927, Dirac devised second quantization to quantize the radiation field and showed how that accounted for photons and radiative transitions.

Although Heisenberg set out to restrict the new theory to observable quantities, this proved to be elusive and the physical meaning of the mathematical formalism has been controversial to this day. The “Copenhagen interpretation” of quantum mechanics was developed in that city by Bohr and Heisenberg working both in collaboration and independently. The famous outcome was Bohr’s principle of complementarity and Heisenberg’s uncertainty principle, both published in 1927. Another and related early landmark was J. von Neumann’s *Mathematische Grundlagen der Quantenmechanik*, Springer (1932). Einstein’s critique of the Copenhagen interpre-

¹That Bose and Fermi statistics require, respectively, symmetric and antisymmetric wave functions was discovered at the same time by Dirac.

tation culminated in the 1935 paper with Boris Podolsky and Nathan Rosen (see §12.1).

In the period 1927–1934 relativistic quantum theory was developed, and this will be sketched in chapter 13.



Enrico Fermi, Werner Heisenberg and Wolfgang Pauli
Photograph by F.D. Rasetti



James Franck and Max Born (with Born's son Gustav)



Arthur H. Compton



P.A.M. Dirac

Photo by A. Börtzells Tryckeri



Erwin Schrödinger

Photo by Francis Simon



Otto Stern

All pictures courtesy of the AIP Emilio Segrè Visual Archives

1.4 Problems

1. Derive Eq. 39 for the two-particle interference pattern produced by finite apertures.

Endnotes

For an instructive discussion of various neutron interference experiments, see D.M. Greenberger, *Rev. Mod. Phys.* **55**, 875 (1983). Remarkable coherence phenomena also arise in one-particle states describing particles possessing “internal” quantum numbers that have no classical counterpart. The most famous and extensively explored examples arise from

neutral K mesons, and in particular, the phenomenon of “regeneration.” In this case there is, however, a clear analogy with coherence phenomena in classical optics – for example, the propagation of polarized light through a magnetized medium. Neutral K meson phenomena are discussed in all books on particle physics; the analogy with propagation in a magnetized medium is in K. Gottfried and V.F. Weisskopf, *Concepts of Particle Physics*, Vol. I, Oxford University Press (1984); p. 152.

§1.2 is drawn from D.M. Greenberger, M.A. Horne and A. Zeilinger, *Physics Today*, pp. 22–29, August 1993, and from K. Gottfried, *Am. J. Phys.* **68**, 143 (2000). These articles cite additional literature.

The key original papers by Heisenberg, Born, Jordan, Dirac and Pauli, translated into English as necessary, on what began as matrix mechanics, together with invaluable comments, appear in B.L. van der Waerden (ed.), *Sources of Quantum Mechanics*, North-Holland (1967), Dover (1968). English translations of Schrödinger’s papers are in E. Schrödinger, *Collected Papers on Wave Mechanics*, Blackie and Son (1928). Dirac’s paper on the quantization of the electromagnetic field is reproduced in J. Schwinger (ed.), *Quantum Electrodynamics*, Dover (1958). English translations of Bohr’s and Heisenberg’s first papers on complementarity and uncertainty appear in J.A. Wheeler and W.H. Zurek (eds.), *Quantum Theory and Measurement*, Princeton University Press (1983), and so does the article by Bohr and Rosenfeld on the measurement of electromagnetic field strengths. The English translation of von Neumann’s book was published by Princeton University Press in 1955.

For technical historical monographs, see E.T. Whittaker, *A History of the Theories of Aether and Electricity*, Vol. 2, Thomas Nelson and Sons (1953); M. Jammer, *The Conceptual Development of Quantum Mechanics*, McGraw-Hill (1966); and S.S. Schweber, *QED and the Men who Made it*, Princeton University Press (1994). For summaries more detailed than given here see A. Pais, *Inward Bound*, Oxford University Press (1986); S. Weinberg, *The Quantum Theory of Fields*, Vol. 1, chapter 1, Cambridge University Press (1995); and H.A. Bethe in *More Things in Heaven and Earth*, B. Bederson (ed.), Springer (1999), or *Rev. Mod. Phys.* **71**, S1 (1999). The historical development of quantum mechanics can also be inferred from the extensive citations in W. Pauli, *Die allgemeine Prinzipien der Wellenmechanik*, Encyclopedia of Physics, Vol. 5, Springer (1955), which is identical to *Handbuch der Physik*, Vol. 24, Part 1, Springer (1933). For the best eyewitness account see W. Pauli, *Scientific Correspondence*, Vol. 1, A. Hermann, K. v. Meyenn and V.F. Weisskopf (eds.), Springer-Verlag (1979).

Original papers on the Old Quantum Theory appear in D. ter Haar, *The Old Quantum Theory*, Pergamon (1967); those most directly relevant to the discovery of matrix mechanics are in van der Waerden (*loc. cit.*). A collection of excerpts from landmark papers, with commentaries, appear in *100 Years of Planck’s Quantum*, I. Duck and E.C.G. Sudarshan, World Scientific (2000). For the role of black body radiation see T. Kuhn, *Blackbody Theory and the Quantum Discontinuity*, Oxford University Press (1978); A. Pais, *Subtle is the Lord . . .*, Oxford University Press (1982); and *Einstein’s Miraculous Year*, J. Stechel (ed.), Princeton University Press (1998), pp. 165–177. A recent discussion of developments at the turn of the last century, with references, appears in R.D. Purrington, *Physics in the Nineteenth Century*, Rutgers University Press (1997), chapter 8.

use in the propagator, that is, in terms of specified initial and final coordinates and the elapsed time, not in terms of the initial coordinates and velocities.

The Lagrangian of interest is

$$L = \frac{1}{2}(\dot{Q}^2 - Q^2) - f(t)Q, \quad (166)$$

where $Q(t)$ is the classical coordinate in dimensionless form, the equation of motion being $\ddot{Q} + Q + f = 0$. Then

$$S_{cl} = \int_{t_a}^{t_b} dt L = \int_{t_a}^{t_b} dt \left(\frac{1}{2} \left[\frac{d}{dt}(Q\dot{Q}) - Q\ddot{Q} - Q^2 \right] - fQ \right) \quad (167)$$

$$= \frac{1}{2}[(Q\dot{Q})_{t_b} - (Q\dot{Q})_{t_a}] - \frac{1}{2} \int_{t_a}^{t_b} dt f(t)Q(t). \quad (168)$$

In the unforced case, the solution of the equations of motion is

$$Q(t) = Q_a \cos(t - t_a) + \dot{Q}_a \sin(t - t_a), \quad (169)$$

where $Q(t_a) = Q_a$, $\dot{Q}(t_a) = \dot{Q}_a$. The propagator requires the action for specified initial and final coordinates given the elapsed time $(t_b - t_a) = T$. Hence the initial and final velocities are

$$\dot{Q}_a = (Q_b - Q_a \cos T) / \sin T; \quad \dot{Q}_b = (-Q_a + Q_b \cos T) / \sin T. \quad (170)$$

Equation (168) then gives the following result for the unforced case:

$$S_{cl}^{(0)}(b, a) = \frac{1}{\sin(t_b - t_a)} \left[\frac{1}{2}(Q_a^2 + Q_b^2) \cos(t_b - t_a) - Q_a Q_b \right]. \quad (171)$$

The rather long calculation for the driven oscillator is outlined in Prob. 9. The result is

$$\begin{aligned} S_{cl}(b, a) = \frac{m\omega}{\sin \omega T} & \left\{ \frac{1}{2}(x_a^2 + x_b^2) \cos \omega T - x_a x_b \right. \\ & + \frac{x_a}{m\omega} \int_{t_a}^{t_b} dt f(t) \sin \omega(t_b - t) + \frac{x_b}{m\omega} \int_{t_a}^{t_b} dt f(t) \sin \omega(t - t_a) \\ & \left. - \frac{1}{m^2 \omega^2} \int_{t_a}^{t_b} dt \int_{t_a}^t ds f(t)f(s) \sin \omega(t_b - t) \sin \omega(s - t_a) \right\}, \end{aligned} \quad (172)$$

where the mass and frequency have been restored, with $f(t)$ now *redefined* by the Lagrangian $\frac{1}{2}m(\dot{x}^2 - \omega^2 x^2) - xf(t)$.

The complete result for the propagator then follows from (165):

$$K(b, a) = \sqrt{\frac{m\omega}{2\pi i \hbar \sin \omega T}} \exp \left(\frac{i}{\hbar} S_{cl}(b, a) \right). \quad (173)$$

In the unforced case, the energy eigenfunctions in the coordinate representation can be found from this propagator; see Prob. 11.

4.3 Motion in a Magnetic Field

The motion of charged particles in electromagnetic fields is a central feature of many phenomena. In classical physics the problem of finding the trajectories can only be solved analytically for a very restricted set of field configurations, and it does not become easier in quantum mechanics. Here only the most important soluble situation will be treated, that of a spatially uniform static magnetic field. Nevertheless, this is a rich problem with many practical applications, especially in condensed matter physics. While classical physics offers an intuitive understanding of what quantum mechanics has to say about motion in a magnetic field, quantum mechanics predicts a startling effect that has no classical counterpart: under appropriate circumstances a charged particle can display interference phenomena produced by a magnetic field that it *never* encounters. This is the Aharonov-Bohm effect, which will also be described in this section.

(a) Equations of Motion and Energy Spectrum

The Hamiltonian for a particle of charge e and mass m in a static magnetic field described by the vector potential \mathbf{A} is

$$H = \frac{1}{2m} \left(\mathbf{p} - \frac{e}{c} \mathbf{A}(\mathbf{q}) \right)^2 . \quad (174)$$

Here \mathbf{p} is the *canonical* momentum; the velocity is *not* \mathbf{p}/m , but rather

$$\mathbf{v} = \frac{1}{m} \left(\mathbf{p} - \frac{e}{c} \mathbf{A} \right) . \quad (175)$$

That is, from (174) and the canonical commutation rules, it follows that the velocity and coordinate are related as claimed in (175):

$$\mathbf{v}(t) = [\mathbf{q}(t), H]/i\hbar . \quad (176)$$

Consequently, the Hamiltonian is also

$$H = \frac{1}{2} m |\mathbf{v}|^2 . \quad (177)$$

Despite appearances, this is not the energy of a free particle as \mathbf{v} does not obey the commutation rules of \mathbf{p}/m . The fundamental commutation rule of this problem follows from $[p_i, A_j] = (\hbar/i) \partial A_j / \partial q_i$:

$$[v_i, v_j] = i \frac{e\hbar}{cm^2} \epsilon_{ijk} B_k , \quad (178)$$

where B_k is a component of the magnetic field.

The velocity commutation rule (178) is gauge-independent — it contains only \mathbf{B} . Equation (177) is a gauge-invariant expression for the energy, and it is best to work with explicitly gauge invariant expressions when possible.

Equation (178) leads directly to the equation of motion for \mathbf{v} :

$$\dot{\mathbf{v}} = \frac{e}{2mc} [\mathbf{v} \times \mathbf{B} - \mathbf{B} \times \mathbf{v}] . \quad (179)$$

When \mathbf{B} is not uniform,

$$[B_j, v_k] = \frac{1}{m} [B_j, p_k] = \frac{i\hbar}{m} \frac{\partial B_j}{\partial q_k}, \quad (180)$$

and the equation of motion in the general case is therefore

$$\frac{d\mathbf{v}}{dt} = \frac{e}{mc} (\mathbf{v} \times \mathbf{B}) + i \frac{e\hbar}{2cm^2} \nabla \times \mathbf{B}. \quad (181)$$

The last term is absent in the classical case, but when the field is uniform Heisenberg's equation is identical to the classical equation of motion.

Consider now the case of a *uniform field*, namely, $\mathbf{B} = (0, 0, B)$, where $B > 0$. The only nonzero commutator among the velocity components is then

$$[v_x, v_y] = i \frac{e\hbar B}{cm^2}. \quad (182)$$

In the light of this, it is best to write the Hamiltonian in terms of the Cartesian components of velocity:

$$H = \frac{1}{2} m (v_x^2 + v_y^2 + v_z^2). \quad (183)$$

Now $v_z = p_z/m$, and commutes with v_x and v_y ; *the momentum parallel to the field is a constant of motion*, just as in classical physics. The motion along \mathbf{B} is simply that of a free particle and can be set aside until needed.

For that reason we only concern ourselves with motion in the x - y plane perpendicular to \mathbf{B} , for which the Hamiltonian is

$$H = \frac{1}{2} m (v_x^2 + v_y^2). \quad (184)$$

The velocity components v_x and v_y do not commute with each other or with H . But according to (182), their commutator is a c-number. Consequently, *the Hamiltonian (184) for motion perpendicular to \mathbf{B} is that of a simple harmonic oscillator!* To see this explicitly, define the operators

$$a = \sqrt{\frac{m}{2\hbar\omega_c}} (v_x + iv_y), \quad a^\dagger = \sqrt{\frac{m}{2\hbar\omega_c}} (v_x - iv_y), \quad (185)$$

where ω_c is the *cyclotron frequency*:

$$\omega_c = \frac{eB}{mc}. \quad (186)$$

A short calculation leads to the same commutation rule as for the operators of the same name in the theory of the harmonic oscillator, i.e.,

$$[a, a^\dagger] = 1. \quad (187)$$

In terms of them, the Hamiltonian for motion in the plane transverse to \mathbf{B} is

$$H = \hbar\omega_c (a^\dagger a + \frac{1}{2}). \quad (188)$$

The energy spectrum for motion of a charged particle in a uniform magnetic field is therefore

$$E_n = \hbar\omega_c (n + \frac{1}{2}), \quad n = 0, 1, \dots \quad (189)$$

These are the *Landau levels*.

From the theory of the oscillator (see Eq. 59) it follows that the characteristic length in the problem is

$$l_B = \sqrt{\hbar/m\omega_c} = \sqrt{\hbar c/eB}. \quad (190)$$

This is called the *magnetic length*. For the electron¹

$$\hbar\omega_c = 1.158 \times 10^{-4} \text{ eV}(B/\text{T}), \quad l_B/a_0 = 4.85 \times 10^2 (B/\text{T}), \quad (191)$$

where $a_0 = 4\pi\hbar^2/me^2$ is the Bohr radius and B/T means the magnetic field in units of tesla (T), or 10^4 gauss. The characteristic velocity of the state with energy E_n is therefore $(v/c)^2 \sim 5 \times 10^{-10} (B/\text{T}) n$.

When the field is uniform, the equation of motion (181) simplifies to

$$\dot{v}_x = \omega_c v_y, \quad \dot{v}_y = -\omega_c v_x. \quad (192)$$

The solution has the same appearance as in the classical case, i.e., for $e > 0$, clockwise circular motion with angular frequency ω_c :

$$x(t) = x_0 - \frac{1}{\omega_c} v_y(t), \quad y(t) = y_0 + \frac{1}{\omega_c} v_x(t). \quad (193)$$

The putative coordinates of the center, (x_0, y_0) , are not c-numbers, however, because of the nonzero velocity commutator:

$$[x_0, y_0] = -il_B^2. \quad (194)$$

Another short calculation will confirm that x_0 and y_0 are constants of motion,

$$[H, x_0] = [H, y_0] = 0, \quad (195)$$

but because of (194), only one can be diagonalized simultaneously with the energy. In classical mechanics, the radius of the orbit is proportional to the energy. The same relation holds for the operators, namely

$$R^2 \equiv [x(t) - x_0]^2 + [y(t) - y_0]^2 = \frac{2}{m\omega_c^2} H. \quad (196)$$

Hence R^2 has a sharp value $(r^2)_n$ in an energy eigenstate,

$$(r^2)_n = (2n + 1)l_B^2; \quad (197)$$

the radii of the stationary states therefore grow like \sqrt{n} .

(b) *Eigenstates of Energy and Angular Momentum*

It is clear that the Landau levels must be highly degenerate. The system is two-dimensional, and the Hilbert space must go over to that of a free particle in two

¹In comparing this section with the literature, note that for the electron $e = -|e|$ in our expressions, whereas some authors set $e \rightarrow -e$ from the outset. Of course, in the numerical values for $\hbar\omega_c$ and l_B , e means $|e|$!

dimensions when $B \rightarrow 0$, which they would not if the states were really just those of a one-dimensional oscillator. The same conclusion can be drawn from the more intuitive remark that in the classical case the orbits for a given energy E are the circles of radius $\sqrt{2E/m\omega_c^2}$ with centers *anywhere* in the transverse plane. Indeed, this implies that the Landau levels must be infinitely degenerate. As we shall see, there are several distinct ways in which these states can be differentiated. One is in terms of angular momentum, which will be developed now. It should be mentioned here that this richness of descriptions of the Landau levels plays a central role in the theory of the quantum Hall effect.¹

To specify states uniquely, one quantum number beyond energy must be given. This quantum number, and the corresponding wave functions, are gauge-dependent to an astonishing degree. One can, as we shall do, choose a gauge in which L_z , the angular momentum along \mathbf{B} , and the energy commute. In this description *the subspace for a given energy is spanned by a discrete infinity of angular momentum eigenstates all centered about the point used to define the angular momentum*. In another popular choice (see Prob. 17), the energy and one linear combination of x_0 and y_0 is diagonalized simultaneously, and this leads to a *continuum* of states of a definite energy localized about all the points on a line in the x - y plane. Both of these descriptions make a subspace of the x - y plane exceptional, and then compensate for this by means of wave functions which are rather weird. Neither has a direct connection to the circular orbits of the classical theory, and for that reason they do not provide an easily visualizable description of the motion. To get a basis that does one must abandon the energy eigenstates in favor of time-dependent coherent states, which will be done in the next subsection.

A description in terms of angular momentum states requires the gauge to be symmetric about \mathbf{B} . Choose $\mathbf{A} = \frac{1}{2}(\mathbf{B} \times \mathbf{r})$, or

$$A_x = -\frac{1}{2}yB, \quad A_y = \frac{1}{2}xB; \quad (198)$$

the velocity components are then

$$v_x = \frac{1}{m}p_x + \frac{\omega_c}{2}y, \quad v_y = \frac{1}{m}p_y - \frac{\omega_c}{2}x. \quad (199)$$

The angular momentum along \mathbf{B} (as always in units of \hbar) is

$$L_z = (xp_y - yp_x)/\hbar. \quad (200)$$

A bit of algebra then gives the Hamiltonian

$$H = \frac{1}{2m}(p_x^2 + p_y^2) + \frac{1}{8}m\omega_c^2(x^2 + y^2) - \frac{1}{2}\hbar\omega_c L_z. \quad (201)$$

As expected L_z is a constant of motion.

The expression $H + \frac{1}{2}\hbar\omega_c L_z$ is the Hamiltonian of an isotropic two-dimensional oscillator of frequency $\frac{1}{2}\omega_c$. The spectrum of this oscillator is $\frac{1}{2}\hbar\omega_c(n_x + n_y + 1)$, where n_x and n_y are 0, 1, ... But n_x and n_y cannot be specified in a representation

¹For an introduction to this topic, see R. Shankar, *Quantum Mechanics*, 2nd ed., Plenum (1994), pp. 587–592.

in which L_z is diagonal, though $n_x + n_y = n_\perp$ can be specified together with μ , the eigenvalue of L_z . This then gives the following formula for the energies:

$$E(n_\perp, \mu) = \frac{1}{2} \hbar \omega_c (n_\perp - \mu + 1). \quad (202)$$

On the other hand, we know that the energies are given by the Landau formula (189), and furthermore, that the energy cannot depend on μ because all axes of rotation perpendicular to the x - y plane are physically equivalent when the field is uniform. Hence (202), while correct, is awkward.

In short, what is desired is a basis $|n, \mu\rangle$ where n is the quantum number in Landau's formula. Motivated by the theory of the harmonic oscillator, we seek operators that manufacture *all* these eigenstates from just one, the state with lowest energy ($n = 0$) and zero angular momentum, $\mu = 0$.

The operator a^\dagger raises n by one. What is still needed are operators that change μ while leaving n fixed. Now recall from §3.5(d) that for any vector operator \mathbf{V} , the combination $V_x + iV_y$ raises the eigenvalue of L_z by one, while $V_x - iV_y$ lowers it by one. As the sought-for vector operators are not to change the energy, they must be constants of motion. Two such operators have already been identified: the center-of-the-circle coordinates (x_0, y_0) . In the gauge (198),

$$x_0 = \frac{1}{2}x + \frac{1}{m\omega_c}p_y, \quad y_0 = \frac{1}{2}y - \frac{1}{m\omega_c}p_x. \quad (203)$$

Define the dimensionless operators

$$Q_\pm = \frac{1}{\sqrt{2}l_B} (x_0 \pm iy_0) = \frac{1}{\sqrt{2}l_B} \left(\frac{x \pm iy}{2} \mp i \frac{p_x \pm ip_y}{m\omega_c} \right). \quad (204)$$

When acting on the eigenstates of H and L_z , they therefore produce

$$Q_\pm |n, \mu\rangle = C_\pm |n, \mu \pm 1\rangle. \quad (205)$$

The coefficients are determined by requiring the states to have norm 1,

$$|C_+|^2 = \langle n, \mu | Q_- Q_+ | n, \mu \rangle = |C_-|^2 + 1, \quad (206)$$

where the last relation follows from (194), or equivalently,

$$[Q_-, Q_+] = 1. \quad (207)$$

From (203), (201) and (194),

$$Q_- Q_+ = \frac{1}{\hbar \omega_c} H + L_z + \frac{1}{2}, \quad (208)$$

and therefore $|C_+|^2 = n + \mu + 1$. With an appropriate choice of the arbitrary phases we thus conclude that

$$Q_+ |n, \mu\rangle = \sqrt{n + \mu + 1} |n, \mu + 1\rangle, \quad (209)$$

$$Q_- |n, \mu\rangle = \sqrt{n + \mu} |n, \mu - 1\rangle. \quad (210)$$

The last equation determines the angular momentum spectrum for every Landau level, because $Q_- |n, -n\rangle = 0$ implies

$$\mu = -n, -n + 1, -n + 2, \dots \quad (211)$$

In words, *the angular momentum spectrum in the degenerate subspace of energy E_n is bounded from below, and takes on the integer values $\mu = -n, -n+1, \dots$* . This statement pertains to particles with positive charge; for a particle with negative charge, like the electron, the angular momentum is bounded from above at $\mu = n$.

The energy raising operator a^\dagger is proportional to

$$v_x - iv_y = \frac{1}{m}(p_x - ip_y) + \frac{i\omega_c}{2}(x - iy), \quad (212)$$

and it therefore *lowers* the eigenvalue of L_z by one.¹ The action of a and a^\dagger on the basis is therefore

$$a^\dagger|n, \mu\rangle = \sqrt{n+1}|n+1, \mu-1\rangle, \quad a|n, \mu\rangle = \sqrt{n}|n-1, \mu+1\rangle, \quad (213)$$

where the coefficients are the same as for the ordinary oscillator because the commutation rule is the same. Consequently,

$$\frac{1}{\sqrt{n!}}(a^\dagger)^n|0, 0\rangle = |n, -n\rangle. \quad (214)$$

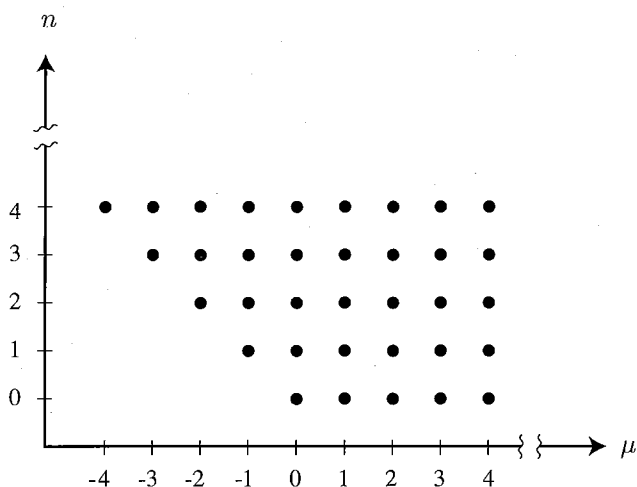


FIG. 4.2. The energy and angular momentum spectra for the motion of a charged particle in a uniform magnetic field; $E_n = \hbar\omega_c(n + \frac{1}{2})$, where ω_c is the cyclotron frequency.

The operators that produce the whole spectrum (see Fig. 4.2) from the state $|0, 0\rangle$ are then the direct extensions of those for the one-dimensional oscillator:

$$|n, \mu\rangle = \frac{1}{\sqrt{n!(n+\mu)!}}(Q_+)^{n+\mu}(a^\dagger)^n|0, 0\rangle. \quad (215)$$

¹Observe that $v_x - iv_y$ is a lowering operator for L_z even though v_x and v_y are linear combinations of canonical coordinates and momenta along different directions. For further discussion of this issue, see Prob. 15.

The wave functions can be found by the technique used for the oscillator (see Prob. 16). The one for $n = \mu = 0$ is

$$\Psi_{00}(\rho) = \frac{1}{\sqrt{2\pi}} e^{-\rho^2/4}, \quad (216)$$

where ρl_B is the radial distance in cylindrical coordinates. The other wave functions can then be generated from this one by differentiation. As already mentioned, *all these states single out the point $\rho = 0$, whereas there is no preferred point in the x - y plane.* The coherent states that will now be constructed do not suffer from this defect.

(c) Coherent States

As in the case of the one-dimensional oscillator, in this problem the coherent states are a complete but non-orthogonal set of time-dependent states, each of which describes the wave packet (216) moving along a classical trajectory *without distortion*. Four real parameters are needed to describe such a trajectory: the radius of the circle, or equivalently, the energy; the point on the circle where the particle is at $t = 0$; and the coordinates of the circle's center.

We have already identified the operators related to motion on the circle, a and a^\dagger ; and those related to the circle's position, Q_\pm . Because each of these pairs satisfies the algebra of creation and destruction operators, and $[a, Q_\pm] = 0$, we can simply copy the theory of the oscillator coherent states for each pair. That is, we introduce two complex numbers, z and w , as the eigenvalues of the destruction operators:

$$(a - z)|z, w\rangle = 0, \quad (Q_- - w)|z, w\rangle = 0. \quad (217)$$

By analogy with the theory of the oscillator, we can anticipate that $|z|^2$ will be proportional to the mean energy, and that w will specify the mean coordinates of the circle's center.

Now there will be two unitary shift operators, one for each pair of creation and destruction operators:

$$D(z) = \exp[za^\dagger - z^*a], \quad F(w) = \exp[wQ_+ - w^*Q_-]; \quad (218)$$

they commute with each other. The coherent states $|z, w\rangle$ are built from the energy and angular momentum eigenstate $|0, 0\rangle$ with eigenvalues $n = \mu = 0$ by replaying Eq. 123:

$$|w, z\rangle = F(w)D(z)|0, 0\rangle. \quad (219)$$

The time development of these states is almost identical to that of the oscillator; namely, $z \rightarrow ze^{-i\omega_c t}$ as before, but w does not change because Q_\pm are constants of motion. Hence,

$$e^{-iHt}|z, w\rangle = |ze^{-i\omega_c t}, w\rangle, \quad (220)$$

where an overall and irrelevant phase $e^{-i\omega_c t/2}$ has again been dropped by defining zero to be the ground-state energy. Let \bar{A} denote the expectation value of A in the state (220). According to (217) and (185),

$$\bar{a}(t) = ze^{-i\omega_c t} = \sqrt{m/2\hbar\omega_c} [\bar{v}_x(t) + i\bar{v}_y(t)]. \quad (221)$$

Setting $z = |z|e^{i\phi}$, we have

$$\bar{v}_x(t) = \sqrt{2\hbar\omega_c/m} |z| \cos(\omega_c t - \phi), \quad \bar{v}_y(t) = -\sqrt{2\hbar\omega_c/m} |z| \sin(\omega_c t - \phi). \quad (222)$$

The expectation value of the energy then follows from (184),

$$\bar{H} = \hbar\omega_c |z|^2, \quad (223)$$

and the mean square radius from (196),

$$\langle R^2 \rangle = 2l_B^2 |z|^2. \quad (224)$$

The expectation value of the circle's center is found from

$$\bar{Q}_- = w = \frac{1}{\sqrt{2}l_B} (\bar{x}_0 - i\bar{y}_0). \quad (225)$$

Combining this with (193) then gives

$$\bar{x}(t) = \sqrt{2}l_B [\operatorname{Re} w + |z| \sin \omega_c t] \quad (226)$$

$$\bar{y}(t) = \sqrt{2}l_B [-\operatorname{Im} w + |z| \cos \omega_c t], \quad (227)$$

where the origin of t was chosen to eliminate the phase ϕ . As promised, this is clockwise motion on a circle whose radius is proportional to $|z|$, and whose central coordinates are proportional to the real and imaginary parts of w (see Fig. 4.3).

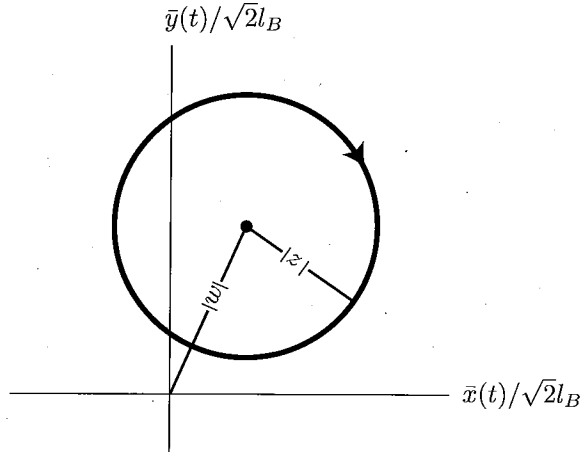


FIG. 4.3. The coherent state description of motion in a homogeneous magnetic field. These states are wave packets that move with constant angular frequency ω_c and without distortion on fixed circles. The complex parameter w specifies the position of the center of the circle, while $ze^{-i\omega_c t}$ gives the instantaneous mean position of the packet on such a circle. As intuition would indicate, the mean energy is proportional to $|z|^2$.

In the discussion of the time-energy uncertainty relation in §2.4(d), we used motion in a uniform magnetic field to illustrate how a system can serve as a clock. The coherent states form the ideal clock in this instance, because they always

keep the minimum size l_B of the lowest state (216). Their angular uncertainty is thus $\Delta\theta \sim l_B/(\langle R^2 \rangle)^{1/2} \sim (\hbar\omega_c/\bar{H})^{1/2}$. The energy uncertainty in a coherent state is $\sim (\hbar\omega_c\bar{H})^{1/2}$, and the time uncertainty, defined as before, is $\Delta T = \Delta\theta/\omega_c$. Consequently for the coherent states $\Delta T \Delta E \sim \hbar$, i.e., the time-energy uncertainty is also minimal for all of these states.

The scalar product and completeness relation satisfied by the coherent states in a magnetic field are the obvious extensions of those in §4.2(c):

$$|\langle z'w'|z, w \rangle|^2 = e^{-|z-z'|^2} e^{-|w-w'|^2}, \quad (228)$$

$$1 = \frac{1}{\pi^2} \int d^2z \int d^2w |z, w \rangle \langle z, w|. \quad (229)$$

(d) The Aharonov-Bohm Effect

In classical electrodynamics, the motion of a charged particle is ultimately determined by the Lorentz force which is only a function of the field strengths at the instantaneous position of the particle, with the potentials being irrelevant. In quantum mechanics the behavior of the particle is determined by its wave function, which is the solution of a Schrödinger equation, and in it the potentials do appear. One might suppose that the gauge invariance of Schrödinger's equation must mean that the potentials themselves are merely a mathematical intermediary, and as in classical physics all observable effects only depend on field strengths "actually experienced" by the particle. That turns out to be false: *if the paths that combine to form the quantum mechanical amplitude do not cross any region in which there is a magnetic field, but surround a region in which there is a field, there are observable phenomena which depend on the magnetic flux enclosed by these paths.* The Aharonov-Bohm effect is the original and best known example of such a phenomenon.

Consider the setup shown in Fig. 4.4, in which a charged particle can reach a detection screen by traversing one or another of two paths on which it cannot encounter a magnetic field, but between which there is a field \mathbf{B} confined to a region between these paths. This field could, for example, be produced by a solenoid carrying a current \mathbf{j} surrounded by an impenetrable cylinder so that the wave function vanishes in the region where $\mathbf{B} \neq 0$. The vector potential, being the solution of $\nabla^2 \mathbf{A} = -\mathbf{j}$, is non-vanishing everywhere, and therefore alters the wave function relative to what it would be when there is no current.

The path integral gives the best insight into the effect. When the magnetic field vanishes everywhere, the Lagrangian in the path integral is that for a free particle, and it will produce the amplitude for detecting a particle at D as the sum of two distinct terms,

$$\Psi(D) = \Psi_{P_1}(D) + \Psi_{P_2}(D), \quad (230)$$

where Ψ_{P_i} is the contribution from the classical path P_i and its immediate neighbors. When the field is turned on, the Lagrangian changes by

$$\Delta L = \frac{e}{c} \mathbf{v} \cdot \mathbf{A}. \quad (231)$$

Each path then acquires an extra factor

$$\exp \left\{ \frac{ie}{\hbar} \int_{t_a}^{t_b} dt \Delta L \right\} = \exp \left\{ \frac{ie}{\hbar c} \int_{t_a}^{t_b} dt \frac{d\mathbf{r}}{dt} \cdot \mathbf{A} \right\} = \exp \left\{ \frac{ie}{\hbar c} \int_{P_i} d\mathbf{r} \cdot \mathbf{A} \right\}. \quad (232)$$

such states. One example of such a state is Eq. 203, which could model the radiation by a classical current of fixed amplitude but random phase.

The last expression for p_n shows that the function $\wp(z)$ is *not* a probability distribution in general, for were it to always satisfy the condition $\wp \geq 0$, it would follow that in all states $p_n \neq 0$ for all n . Hence any state with a finite number of photons does not have a positive semi-definite \wp , and for such states \wp cannot be interpreted as a probability distribution. This is not too surprising, because in §4.2(d) we learned that the integration over the z -plane corresponds to an integration over phase space, and it is not possible, in general, to define a quantum mechanical phase space distribution. In fact, there is a relationship between \wp and the Wigner phase space distribution (§2.2(f)); recall that the latter is also not positive definite in general.

There are, however, important states of the field for which \wp is a probability distribution. For example, the field produced by a source whose amplitude A is definite but phase is random can be represented in the form of (199) with

$$\wp(z) = \frac{1}{2\pi A} \delta(A - |z|). \quad (203)$$

Another very important example is *black body radiation*, for which the density matrix of the field will be derived in §11.3. The modes are uncoupled, and the complete density matrix is a direct product over all modes of

$$\rho_k = (1 - e^{-\beta\omega}) \sum_{n=0}^{\infty} e^{-n\beta\omega} |n\rangle\langle n|, \quad (204)$$

where $\omega = |k|$, $\beta = 1/k_B T$, and k_B is Boltzmann's constant. The mean occupation number is given by the Planck distribution law,

$$\bar{N}_k = \frac{1}{e^{\beta\omega} - 1}, \quad (205)$$

and therefore the probability of finding n photons in the mode k is

$$p_n = \frac{(\bar{N}_k)^n}{(1 + \bar{N}_k)^{n+1}} \rightarrow \frac{1}{\bar{N}_k}, \quad \bar{N}_k \gg 1. \quad (206)$$

The dispersion in N , whose evaluation is left as an exercise, is

$$\Delta N_k = \sqrt{\bar{N}_k(\bar{N}_k + 1)} \rightarrow \bar{N}_k, \quad \bar{N}_k \gg 1. \quad (207)$$

This is to be compared with the result for the coherent state (Eq. 198); briefly put, thermal radiation has a far broader distribution than does the radiation from an ideal laser.

As a consequence of (202), thermal radiation has a Gaussian coherent state distribution,

$$\wp(z_k) = \frac{1}{\pi \bar{N}_k} e^{-|z_k|^2 / \bar{N}_k}, \quad (208)$$

as can be confirmed by substituting into (202). Such a Gaussian distribution is characteristic of a chaotic system, and holds for a large variety of light sources.

(c) *Photon Coincidences*

We return to the beam splitter, and first consider the case where an *arbitrary beam* is incident in channel 1, channel 0 is empty, and coincidences between the exit channels 2 and 3 are counted. In the notation of (186),

$$N_2 \doteq |T|^2 N_1 + X, \quad N_3 \doteq |R|^2 N_1 + Y, \quad \langle XY \rangle = -r^2 \langle N_1 \rangle, \quad (209)$$

where the latter follows from (188), and $\langle \dots \rangle$ is the expectation value in the incident state. Then the number of coincidences is

$$\langle N_2 N_3 \rangle = r^2 \{ \langle N_1^2 \rangle - \langle N_1 \rangle \}. \quad (210)$$

The fluctuation in coincidences is

$$\Delta N_2 \Delta N_3 \equiv \langle (N_2 - \langle N_2 \rangle)(N_3 - \langle N_3 \rangle) \rangle = \langle N_2 N_3 \rangle - \langle N_2 \rangle \langle N_3 \rangle. \quad (211)$$

From Eq. 209, $\langle N_2 \rangle \langle N_3 \rangle = r^2 \langle N_1 \rangle^2$, and therefore

$$\Delta N_2 \Delta N_3 = r^2 \{ \langle N_1^2 \rangle - \langle N_1 \rangle^2 - \langle N_1 \rangle \} \quad (212)$$

$$= r^2 \{ (\Delta N_1)^2 - \langle N_1 \rangle \} \quad (213)$$

$$\equiv r^2 Q. \quad (214)$$

This simple result is remarkable, for it shows that this correlations of fluctuations distinguishes between the most important categories of states:

1. When the state incident is chaotic, like black body radiation, $Q = \langle N_1 \rangle^2$, i.e., Q is positive. That Q is positive for an ordinary light beam is responsible for the famous Hanbury Brown-Twiss effect.
2. When it is a coherent state, like that produced by an ideal laser, $Q = 0$.
3. When it is a Fock state, which has no fluctuations in N_1 , then Q is negative.

In the quantum optics literature states of the electromagnetic field for which Q is positive, and more generally for which $\wp(z)$ is non-negative, are called classical, which is a bit confusing as the Planck distribution is hardly classical.

The last state we will consider here has one photon incident in both channels 0 and 1, $n_0 = n_1 = 1$. According to (181), in this case $N_2 \doteq 1 + X$, $N_3 \doteq 1 + Y$, and $\langle XY \rangle = -4r^2$. Using $|T|^2 + |R|^2 = 1$ gives

$$\langle N_2 N_3 \rangle = (|T|^2 - |R|^2)^2. \quad (215)$$

Thus for a 50:50 beam splitter, there are *no coincidences* — *in all events one photon is reflected and the other is transmitted, so that both go to the same counter.*

This astonishing result actually illustrates, yet again, that when a quantum state has two paths for reaching an outcome, and no step is taken to ascertain the path, the amplitudes for these alternatives must be added coherently. To have a coincidence, both photons have to be either reflected or transmitted, and the amplitudes for these two options must be added coherently. Now $T = e^{i\varphi_1}/\sqrt{2}$, $R = e^{i\varphi_2}/\sqrt{2}$ when $|T|^2 - |R|^2 = 0$, and (185) requires $\varphi_1 - \varphi_2 = \frac{1}{2}\pi$. Apart from a common

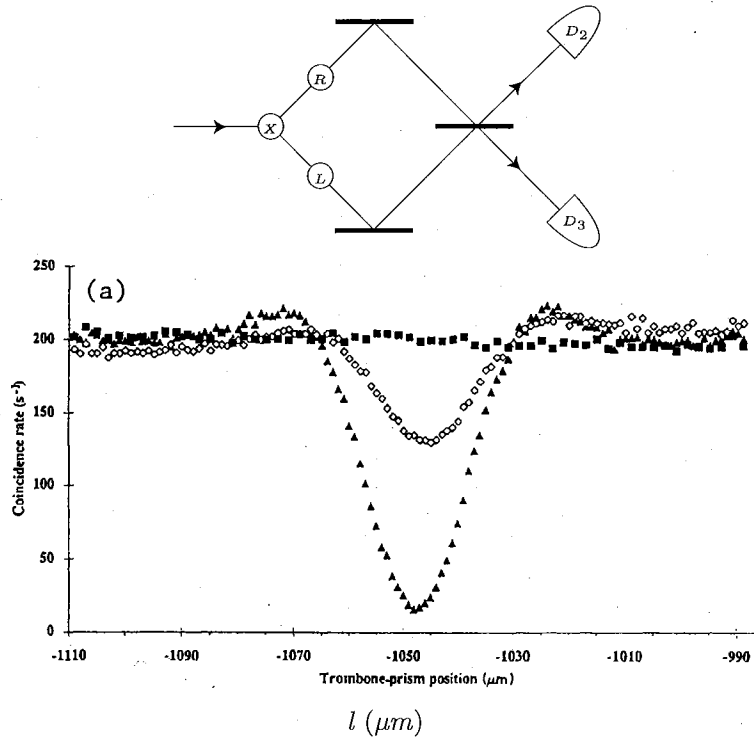


FIG. 10.4. Above, a cartoon version of the experiment by P.G. Kwiat, A.M. Steinberg and R.Y. Chiao, *Phys. Rev. A* **45**, 7729 (1992). The nonlinear crystal X produces two photons polarized in the plane of the page; R rotates the polarization through ϕ ; and L is an optical “trombone” that provides a difference l in the length of the two paths. The coincidence rates as a function of l for $\phi = 0$ (▲), $\frac{1}{4}\pi$ (◊), $\frac{1}{2}\pi$ (■) are shown, demonstrating that the rate vanishes, within experimental errors, at $l = \phi = 0$ and grows as the distinguishability of the paths grows.

phase, the amplitude for the case where both photons are reflected or transmitted is therefore

$$\frac{1}{\sqrt{2}} \times \frac{1}{\sqrt{2}} + \frac{i}{\sqrt{2}} \times \frac{i}{\sqrt{2}} = 0, \quad (216)$$

whereas when one is reflected and the other transmitted the amplitude is

$$\frac{1}{\sqrt{2}} \times \frac{i}{\sqrt{2}} + \frac{i}{\sqrt{2}} \times \frac{1}{\sqrt{2}} = i. \quad (217)$$

An experiment confirming this effect is summarized in Fig. 10.4. It is, of course, no simple matter to produce a state in which one photon in each channel 0 and 1 is incident on the beam splitter in essence simultaneously. The trick is to use a nonlinear crystal, illuminated by a laser, which converts one photon into two having the *same* polarization. The experiment also allows the polarization of *one* of the incident photons to be rotated through an angle ϕ , so when $\phi = \frac{1}{2}\pi$ it becomes possible to *unambiguously* determine the path taken by the photons by measuring their polarization after passage through the beam splitter. In short, as ϕ grows from 0 to $\frac{1}{2}\pi$, the coherence of the amplitudes for the two paths shrinks to zero, and the coincidence rate is expected to increase correspondingly, which it does.

10.6 The Photoeffect in Hydrogen

The photoeffect — the ejection of an electron from an atom, is the basic process underlying most, though not all, means for detecting photons. It therefore offers an instructive and important example of a radiative transition. As we do not yet have a relativistic theory at our disposal for electrons, we are restricted to photon energies well below mc^2 . In addition, we will only treat the photoeffect in hydrogen, but that suffices to bring out some of the most important features of the process.

Energy conservation relates the momenta of the electron and the photon, \mathbf{p} and \mathbf{k} :

$$k - E_0 = p^2/2m, \quad (218)$$

where E_0 is the ground state binding energy, and proton recoil has been ignored (i.e., its mass relative to that of the electron is taken to be infinite). There are two rather distinct energy regimes:

1. $k \gg E_0$. For k well above the threshold at $E_0 = \frac{1}{2}\alpha^2 m$, the velocity of the ejected electron is $v \simeq \alpha\sqrt{k/E_0}$ — i.e., large compared to the velocity α of bound electrons, and for that reason the interaction between the ejected electron and the proton can be ignored.
2. $k - E_0 \lesssim E_0$. The ejected electron's velocity is too low to permit neglect of the Coulomb interaction. To be more precise, the parameter $\gamma = \alpha/v$ that appears in the Coulomb wave functions (recall §8.4(a)) is large in this regime, because

$$\frac{1}{\gamma} = pa_0 = \sqrt{\frac{k}{E_0} - 1}. \quad (219)$$

Nevertheless, the problem is tractable because in the threshold region the photon wavelength λ is of order a_0/α , i.e., enormous compared to the atom's dimension, so only the lowest photon partial wave, with $j = 1$, interacts. That is, in this regime the photoelectron only emerges in a p wave. Furthermore, the low-energy calculation is valid up to $ka_0 \sim 1$, or $k \sim E_0/\alpha \gg E_0$, which overlaps the high-energy regime, and therefore the two calculations give a complete description of the process for all $k \ll m$.

In this whole nonrelativistic regime, the electron's spin can be ignored to leading order in v (see Eq. 137).

(a) High Energies

In the high-energy regime, the photon wavelength is not large compared to the size a_0 of the absorber, and the multipole expansion is not valid. Therefore the phase factor in the vector potential must be retained, and the matrix element for the process is to be taken from (156):

$$\langle \mathbf{p}; 0 | H_1 | 1s; 1_{k\lambda} \rangle = -\frac{e}{m} \frac{1}{\sqrt{2V_k}} (\mathbf{p} \cdot \mathbf{e}_{k\lambda}) \langle \mathbf{p} | e^{i\mathbf{k} \cdot \mathbf{r}} | 1s \rangle, \quad (220)$$

where advantage was taken of the fact that the state $|\mathbf{p}\rangle$ of the photoelectron is a momentum eigenstate. The final factor in (220) is essentially the ground state

correlations if the particles are identical and the temperature is low. As we already know from the example of the ideal gas, this requirement imposes correlations even in the absence of forces.

It is intuitively clear that if the inter-particle forces are strong, there must be much stronger correlations than those imposed by symmetry or antisymmetry. For example, if the interaction has a very strong repulsion for separations smaller than r_0 , the pair correlation function must nearly vanish for such separations. The repulsive correlations imposed by the exclusion principle in an ideal Fermi gas do not meet this requirement, while those in an ideal Bose gas have the opposite effect. Thus it is evident that the mean field approximation can only hope to be accurate if the interactions are, in some sense, weak; what is meant here by "in some sense" will be discussed presently.

The assumption that the force on a particle is to be approximated by the mean field implies that each particle is to move as if it were in an external potential. Therefore it has its "own" wave function, so to say, with the many-body wave function a product of these, though symmetrized or antisymmetrized.

Two many-body systems will be treated here: the dilute Bose-Einstein condensate, and the low-lying states of many electron atoms. By dilute we mean a density low enough so as to make the interaction in effect weak. In the case of atoms, the weak interaction restriction is not met, in fact, but the mean field (or Hartree-Fock) approximation is nevertheless important, for both pedagogical and practical reasons.

(a) *The Dilute Bose-Einstein Condensate*

Even an arbitrarily weak interaction is of crucial importance in a Bose gas. If the interaction is attractive, and has a range r_0 , then the lowest state is one where all particles are collapsed into a microscopic volume of order r_0^3 , giving a negative interaction energy proportional to N^2 that dominates the kinetic energy which is of order N .¹

A weak repulsion also plays a crucial role, as shown by the following argument. Assume the gas is in a rigid enclosure, say a sphere of radius R , with $R^3 \propto N$. The ground-state wave function of one particle in this enclosure is

$$\varphi(r) = \frac{1}{\sqrt{2\pi R}} \frac{1}{r} \sin\left(\frac{\pi r}{R}\right). \quad (141)$$

The ground state wave function of the ideal gas is then

$$\Psi = \prod_{i=1}^N \varphi(\mathbf{r}_i). \quad (142)$$

But this is a preposterous wave function: it states that the gas density is

$$n(r) = \frac{N}{2\pi R} \frac{1}{r^2} \sin^2\left(\frac{\pi r}{R}\right), \quad (143)$$

rather than being uniform except near the boundary.

¹In this section N is the number of particles, and not the number operator.

The function Ψ is only correct when the interaction between particles *vanishes identically*. It minimizes the kinetic energy $K \propto \int \varphi \nabla^2 \varphi$; according to (141), $K \sim N/R^2 \sim N^{\frac{1}{3}} \sim \Omega^{\frac{1}{3}}$, which is vastly smaller than an energy that is proportional to the system's volume. Properties proportional to the volume are called *extensive*, and most systems in nature have energies that are extensive. By contrast, a two body interaction of finite range will, in an extensive system, produce a potential energy proportional to $n^2 \Omega$, which is enormous compared to K . Thus if there is any interaction between the particles, the wave function (142) ceases to bear any resemblance to reality; the correct wave function must produce a density that is uniform except near the walls of an enclosure.¹

This enormous sensitivity to interactions of the free-particle wave function shown by the Bose gas does not occur in the Fermi case. Because of the exclusion principle, the free particle ground state is made up of wave function with wavelengths down to $1/k_F$, which is a distance of order the mean inter-particle spacing, and as a result the density produced by the naive many-body wave function is spatially uniform.

To find a realistic description of the Bose gas, the interaction must be taken into account *ab initio*. We do so for the case of a dilute system, such as the atomic Bose-Einstein gases that have been studied extensively in recent years. The important case of superfluid He^4 is far more difficult because in this system the interaction is far too strong to be handled by the mean field approximation.

In the condensate, the particles move very slowly, so the collisions between them can be described by the *S*-wave scattering length a . The true interaction can then be replaced by the pseudo-potential (Eq. 8.313),

$$v_{12} = \frac{4\pi a}{m} \delta(\mathbf{r}_1 - \mathbf{r}_2), \quad (144)$$

bearing in mind that the reduced mass is $m/2$ in this case. The scattering length must be positive if the system is not to collapse.

The interaction is, in effect, weak if a is small compared to the mean interparticle distance d , where $d^3 = n$ is the mean density. Nevertheless, the true force can have both strong repulsive and attractive components as long as they result in a positive scattering length that is short compared to d . Thus the precise meaning of the term dilute is $d \gg a$. In the second-quantized form (Eq. 44), and the dilute gas approximation, the interaction between the particles is therefore

$$V = \frac{2\pi a}{m} \int d\mathbf{x} \psi^\dagger(\mathbf{x}) \psi^\dagger(\mathbf{x}) \psi(\mathbf{x}) \psi(\mathbf{x}). \quad (145)$$

The mean field approximation assumes that the state of the system can be adequately described by assigning the constituents to one-body states moving in a mean field. In the case of a condensed Bose gas, a finite fraction of all particles occupy the lowest of these states, and at $T = 0$ all are in this state. Let $\phi(\mathbf{x})$ be this lowest one-body wave function; together with the functions $\{u_\nu(\mathbf{x})\}$ it forms a complete orthonormal set that vanishes on the walls of the enclosure. Further, let c and b_ν be the destruction operators for the corresponding one-body states, so that the whole Bose field operator is

$$\psi(\mathbf{x}) = \phi(\mathbf{x}) c + \sum_\nu u_\nu(\mathbf{x}) b_\nu. \quad (146)$$

¹In this connection, see Problem 3.

By hypothesis, the ground state is

$$|G\rangle = \frac{1}{\sqrt{N!}} (c^\dagger)^N |0\rangle. \quad (147)$$

The objective is the expectation value of H in this state. The kinetic and potential energies involve the expressions $\psi(\mathbf{x})|G\rangle$ and $\psi(\mathbf{x})\psi(\mathbf{x})|G\rangle$, and in both only the term ϕc of ψ gives a nonzero contribution because the operators b_ν acting on $|G\rangle$ give zero. When the destruction operator c acts on any function of c^\dagger it can be represented by

$$c = \partial/\partial c^\dagger, \quad (148)$$

and therefore $\langle c^\dagger c \rangle_G = N$, and $\langle c^\dagger c^\dagger c c \rangle_G = N(N-1) \simeq N^2$ when $N \gg 1$. In view of this, we define what is called *the condensate wave function*

$$\Psi(\mathbf{x}) = \sqrt{N} \phi(\mathbf{x}), \quad (149)$$

even though Ψ is not normalized to unity, but to N . In term of Ψ the ground-state energy is thus

$$\mathcal{E}[\Psi] = \int d\mathbf{x} \left\{ -\frac{1}{2m} \Psi^*(\mathbf{x}) \nabla^2 \Psi(\mathbf{x}) + \frac{2\pi a}{m} |\Psi(\mathbf{x})|^4 + U(\mathbf{x}) |\Psi(\mathbf{x})|^2 \right\}, \quad (150)$$

where U is an external potential that represents the enclosure or an optical trap holding the gas.

The equation satisfied by Ψ is found by varying the functional $\mathcal{E}[\Psi]$. Two points must now be borne in mind: (i) the variation must keep $|\Psi|^2$ normalized to N , which is done by varying

$$\mathcal{E}[\Psi] - \epsilon \int d\mathbf{x} |\Psi(\mathbf{x})|^2, \quad (151)$$

where ϵ is a Lagrange multiplier; and (ii) that in general Ψ is complex, and therefore (151) is to be stationary under variations of Ψ and Ψ^* independently. Varying with respect to Ψ^* then gives *the Gross-Pitaevskii equation*,

$$-\frac{1}{2m} \nabla^2 \Psi + \frac{4\pi a}{m} |\Psi|^2 \Psi + U \Psi = \epsilon \Psi. \quad (152)$$

This equation, and even more so its time-dependent generalization, has many interesting solutions beyond the ground state of the condensate.¹ We confine ourselves to the latter, and assume there is no applied force beyond the rigid walls of an enclosure, i.e., $U = 0$ in (152). As in the Schrödinger equation, this ground-state wave function is real. We anticipate, and will shortly confirm, that Ψ is a constant C except near the walls, and that the distance l in which Ψ rises from $\Psi = 0$ at the walls is microscopic. Hence the normalization integral is $C^2 \Omega$, aside from a negligible surface term, and as the integral must equal N we have $C = \sqrt{n}$, where n is the number density. On the other hand, when Ψ is a constant and $U = 0$, (152) reduces to

$$|\Psi(\mathbf{x})|^2 = m\epsilon/4\pi a. \quad (153)$$

¹F. Dalfovo, S. Giorgini, L.P. Pitaevskii and S. Stringari, *Rev. Mod. Phys.* **71**, 463 (1999).

When integrated over space, (153) becomes $N = (m\epsilon/4\pi a)\Omega$, and therefore

$$\epsilon = 4\pi a n / m. \quad (154)$$

If the surface layer is microscopic, the behavior of Ψ near the walls cannot depend on the shape of the enclosure, and it suffices to consider a large box with a wall at the yz -plane, the interior being $x \geq 0$. The behavior of Ψ near this wall is then given by the one-dimensional Gross-Pitaevskii equation

$$\Psi'' + 8\pi a \Psi(n - \Psi^2) = 0. \quad (155)$$

The boundary conditions are

$$\Psi(0) = 0, \quad \Psi(x) \rightarrow \sqrt{n}, \quad x \rightarrow \infty. \quad (156)$$

It is left to the reader to confirm that the desired solution of (155) is

$$\Psi(x) = \sqrt{n} \tanh(x/l), \quad l = 1/\sqrt{4\pi a n} = d\sqrt{d/4\pi a}. \quad (157)$$

As expected the condensate density rises to its constant value in a microscopic distance that is large compared to the interparticle spacing when the system is dilute. Also as expected, this distance shrinks as the effect of the interaction increases, whether due to an increasing scattering length or density.

(b) The Hartree-Fock Equations

In the mean field approximation, the actual many body interaction is mimicked by a one-body "potential," and by the same token, the actual wave function of a system of identical fermions is approximated by an antisymmetrized product of N one particle wave functions. The approximation is made *self-consistent* by requiring the potential acting on a given particle to be the average field produced by all other particles. This averaging is done with the sought-for wave functions, and therefore the self-consistency requirement will lead to non-linear equations for the one-particle wave functions.

Let $\phi_1(1), \dots, \phi_N(N)$ be these one-particle wave functions; in atomic physics they are often called spin-orbitals. They are assumed to be orthonormal. Here the suffix stands for a set of four quantum numbers, e.g., the $(n_1 l_1 j_1 m_1)$ of atomic spectroscopy, and the argument stands for the eigenvalues of four one-particle degrees of freedom, e.g., (\mathbf{r}_1, s_1) , where $s = \pm \frac{1}{2}$ is the spin projection. The ϕ_i are not a complete set, of course, but can be augmented with other functions that will play no more than a brief and purely formal role to make the set complete. Let a_i^\dagger be the creation operator for the one-particle state whose wave function is ϕ_i . Then the N -body state we are working with is

$$|\Phi\rangle = \prod_{i=1}^N a_i^\dagger |0\rangle. \quad (158)$$

That is, the states $i = 1, \dots, N$ have occupation numbers one, and all others are unoccupied.

The mean field approximation amounts to finding the best wave function of this type, where "best" is to be understood in the sense of the variational principle.

Now $f - \gamma$ coincidences between what we call the object and apparatus states have the rate

$$\mathcal{R}(f|\gamma) = \frac{1}{4}\eta^2[1 + 2T \cos(\phi - \delta) + T^2]. \quad (105)$$

This coincidence rate $\mathcal{R}(f|\gamma)$ displays coherence because identifying the states $|\alpha\rangle$ and $|\gamma\rangle$ affects the experiment's ability to distinguish whether an incident photon took a path through one crystal as compared to the other, i.e., whether the initial photon occupied $|1\rangle$ or $|2\rangle$. When $|T| = 1$ the two paths are equally likely, and the interference pattern has maximal visibility. On the other hand, if $T = 0$ the beam splitter BS_2 has been turned into a mirror and it becomes possible, by detecting $|\beta\rangle$, to know with full confidence which path was taken; hence there can be no interference pattern. In short, therefore, this experiment illustrates the general conclusions drawn at the end of the preceding subsection.

The singles rate at the detector D_1 also displays coherence when the two "apparatus" states are identified:

$$\mathcal{R}(f) = \mathcal{R}(f|\beta) + \mathcal{R}(f|\gamma) = \frac{1}{2}\eta^2[1 + T \cos(\phi - \delta)]. \quad (106)$$

That this is to be expected can be seen in (103). When $T = 1$, and thus $R = 0$, there is no entanglement between the apparatus state $|\gamma\rangle$ and object state, so that $|3\rangle$ and $|4\rangle$ are fully coherent and interfere maximally in forming the detected state $|f\rangle$. In this case, therefore, the experiment is in essence reversible – it has an output that is in essence identical with the input, but of course it does not produce any knowledge about the incident photon. As T decreases (and thus R increases) there is growing entanglement and growing knowledge as to whether a incident photon was $|1\rangle$ or $|2\rangle$, and decreasing coherence.

The experimental results are shown in Fig. 12.6, and are in excellent agreement with (106). The variation of the visibility with $|T|$ illustrates that the degree of confidence regarding the state of the apparatus is complementary to the coherence between states of the object.

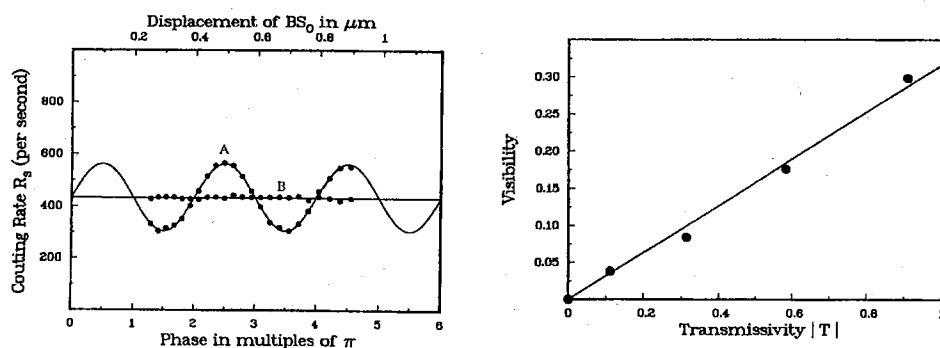


FIG. 12.6. The plot on the left shows the singles rate $\mathcal{R}(f)$ as a function of the phase ϕ , which is varied by moving the beam splitter BS_2 ; the curve A is for $|T| = 0.91$, and B for $|T| = 0$. The right-hand plot shows the visibility (i.e., amplitude) of the interference effect seen in $\mathcal{R}(f)$ as a function of the transmission amplitude $|T|$. In both plots the statistical errors are smaller than the dot size.

This experiment also bears on a famous dictum by Dirac,¹ which reads “[e]ach photon then interferes only with itself. Interference between two different photons never occurs.” The interference between the photons in the channels f and γ demonstrates that this statement only applies to one-photon states, not to multiphoton states, and shows that the superposition principle, whose profound importance was first emphasized by Dirac, has consequences even he may not have fully appreciated.

(d) A Delayed Choice Experiment

Quantum mechanics does not assign values to observables prior to measurement, a feature of the theory that is confirmed by the experiments that violate the Bell-Clauser-Horne inequalities. That measurement does not reveal pre-existing values is also demonstrated by the possibility of leaving the decision “until the last moment” as to which one of two or more incompatible observables is to be measured. The Aspect experiment is such a delayed choice experiment. Another is the two-particle interferometer of §1.2, but that is only a *Gedanken* experiment. An elegant laboratory experiment that is essentially equivalent has been performed by Scully and collaborators. The delayed choice is between determining the path of a photon (in effect its momentum), or foregoing this path information in favor of displaying a two-photon interference pattern.

In this experiment a light beam impinges on a non-linear crystal, in which a single pair of photons is created coherently at one of two spots (see Fig. 12.7). One of these photons triggers the nearby detector D_0 , whereas the other photon passes through an array of 50-50 beam splitters to one of four more distant detectors $D_{1..4}$. Nothing is altered while the photons are in flight, but as we will see this is, in effect, a delayed choice experiment.

Let $|g_i\rangle$ be the ground state of detector i , with $i = 0, \dots, 4$, and define

$$|\Xi\rangle = |0\rangle \otimes |g_0\rangle \otimes \cdots \otimes |g_4\rangle, \quad (107)$$

where $|0\rangle$ is the electromagnetic vacuum state. Schematically, the interaction of the photons with the detectors is

$$V = (a_1 + a_2)\tau_0 + \sum_{\mu=\alpha}^{\delta} a_{\mu}\tau_{\mu} + \text{h.c.}, \quad (108)$$

where a_{μ}^{\dagger} creates a photon in one of the modes α , etc., shown in Fig. 12.5, and τ_{μ} produces the excitation $|f\rangle$ of the corresponding detector: $\tau_{\mu}|g\rangle = |f\rangle$.

Call $|\Psi(t)\rangle$ the state of the system at time t , where the times of special interest are defined in Fig. 12.7. At t_1 photon 1 or 2 has triggered the detector D_0 while another is still in flight, so that

$$|\Psi(t_1)\rangle = \frac{1}{\sqrt{2}}(a_3^{\dagger} + e^{i\phi}a_5^{\dagger})\tau_0|\Xi\rangle, \quad (109)$$

where the phase ϕ accounts for the path difference due to the adjustable position of D_0 . A calculation like the one that led to (101) shows that after the second photon

¹The most recent appearance is on p. 9 of P.A.M. Dirac, *The Principles of Quantum Mechanics*, 4th ed., Oxford (1958).

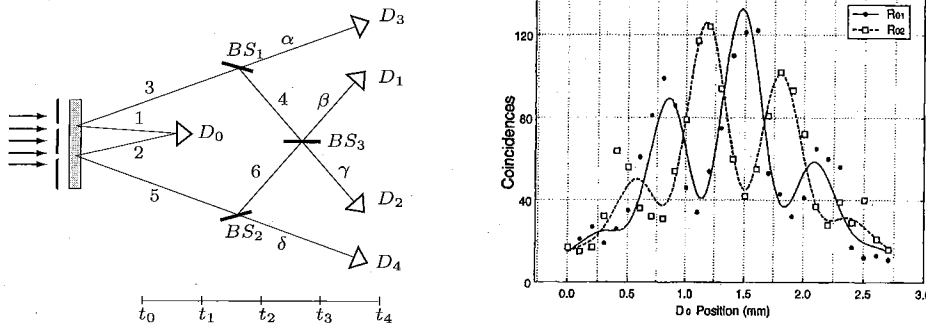


FIG. 12.7. The arrangement of the experiment by Y-Ho. Kim, R. Yu, S.P. Kulik, Y. Shih and M.O. Scully, *Phys. Rev. Lett.*, **84**, 1 (2000) is sketched on the left. The rates R_{01} and R_{02} for detecting one photon in D_0 and another in D_1 or D_2 are shown on the right.

has disappeared the state is

$$|\Psi(t_4)\rangle = \frac{1}{2} \left\{ \tau_3 + e^{i\phi} \tau_4 + \frac{1}{\sqrt{2}} i(1 + ie^{i\phi}) \tau_2 - \frac{1}{\sqrt{2}} (1 - ie^{i\phi}) \tau_1 \right\} \tau_0 |\Xi\rangle. \quad (110)$$

Thus the rates for events in which one photon triggers D_0 , and the other photon subsequently triggers either D_1 or D_2 , are proportional to $|1 \pm ie^{i\phi}|^2$, i.e.,

$$R_{01} = \frac{1}{4}(1 + \sin \phi), \quad R_{02} = \frac{1}{4}(1 - \sin \phi). \quad (111)$$

These are interference patterns between points separated in both space and time. The other two rates show no such interference: $R_{03} = R_{04} = \frac{1}{4}$. The data in Fig. 12.5(b) is consistent with Eq. 111, bearing in mind that the sensitivity of D_0 depends on ϕ , a complication that is ignored in the derivation of (110).

The absence of interference in R_{03} (R_{04}) reflects the fact that in such events it is unambiguous from which spot in the crystal the photon originated that subsequently struck the detector D_3 (D_4). On the other hand, both spots can be the source when D_1 or D_2 is struck, so the two possible paths add coherently.

That the setup in Fig. 12.7 is equivalent to a delayed choice experiment can be seen by considering a somewhat different arrangement.¹ Namely, replace the beam splitters BS_1 and BS_2 by mirrors, and let BS_3 be removed at random. Of course D_3 and D_4 are then decoupled and irrelevant. If “in” and “out” designate the cases where BS_3 is in or out of place, the final states in these two circumstances are

$$|\Psi_{\text{in}}(t_4)\rangle = \frac{1}{2} \left\{ (1 + ie^{i\phi}) \tau_2 + (i + e^{i\phi}) \tau_1 \right\} \tau_0 |\Xi\rangle, \quad (112)$$

$$|\Psi_{\text{out}}(t_4)\rangle = \frac{1}{\sqrt{2}} (\tau_2 + e^{i\phi} \tau_1) \tau_0 |\Xi\rangle. \quad (113)$$

Thus when BS_3 is in place, the amplitudes for triggering D_1 and D_2 are, apart from a common factor, the same as in (110), and therefore the rates R_{01} and R_{02} show the same interference patterns as those in (111). On the other hand, when BS_3 is removed, the rates R_{01} and R_{02} show no interference because the paths are now determined.

¹This is the delayed choice experiment originally proposed by Wheeler (WZ, p. 183).

As in the experiments that test Bell's inequality, the time ordering of events merits comment. In the laboratory frame, D_0 is struck before the other detectors $D_1 \dots D_4$, but the former is at a spacelike separation from the latter. Hence there is no absolute significance to this time sequence; there are frames in which D_0 is struck after the others. An equivalent way of seeing this is to consider a different arrangement in which D_0 , in the frame of Fig. 12.7, is moved far to the right so that it is struck after the others; the rates R_{0i} are unaffected.

(e) Summation

Consider an object \mathcal{O} that possesses an observable Λ with eigenvalues λ_i . The goal is to determine the frequency with which distinct, individual specimens of \mathcal{O} in a state $|\Psi\rangle$ display the eigenvalue λ_i , that is, are "found" to be in the state $|\lambda_i\rangle$. For this purpose there must be an interaction H_c between \mathcal{O} and an apparatus \mathcal{A} that forces the eigenvalues λ_i to be uniquely correlated to the final states of \mathcal{A} . In the input \mathcal{O} and \mathcal{A} are isolated from each other and H_c is inoperative, so that the whole system $\mathcal{O} + \mathcal{A}$ is in an uncorrelated state,

$$|\Theta_{\text{in}}\rangle = |\Phi_{\text{in}}\rangle \otimes |\Psi\rangle, \quad |\Psi\rangle = \sum_i c_i |\lambda_i\rangle, \quad (114)$$

where $|\Phi_{\text{in}}\rangle$ is a state of \mathcal{A} . The unitary transformation generated by such an interaction H_c produces the entangled output state

$$|\Theta_{\text{out}}\rangle = \sum_i c_i |\Phi_i\rangle \otimes |\lambda_i\rangle, \quad (115)$$

where the $|\Phi_i\rangle$ are orthogonal states of \mathcal{A} .

An ideal measurement experiment is one whose output provides an unambiguous macroscopic distinction between these apparatus states $|\Phi_i\rangle$, so that the determination that \mathcal{A} is in the state $|\Phi_i\rangle$ in a particular trial guarantees that the object \mathcal{O} is in the state $|\lambda_i\rangle$ in this trial. Consequently, such a specimen of \mathcal{O} is assigned to the normalized post-measurement state $|\lambda_i\rangle$.

All results of observations on the apparatus can be expressed in terms of its reduced density matrix $\rho(\mathcal{A})$,

$$\rho(\mathcal{A}) = \sum_i \langle \lambda_i | \Theta_{\text{out}} \rangle \langle \Theta_{\text{out}} | \lambda_i \rangle = \sum_i |c_i|^2 P(\Phi_i), \quad (116)$$

where $P(\Phi_i)$ is the projection operator onto $|\Phi_i\rangle$. Although $|\Theta_{\text{out}}\rangle$ is a pure state, $\rho(\mathcal{A})$ is not – it has positive entropy (unless there is just one term in Eq. 114). This is true of *reduced* density matrices quite generally. However, a "good" measurement setup manufactures an output whose *complete* (repeat, complete) density matrix ρ_{out} is, to all intents and purposes, indistinguishable from an effective density matrix ρ_{eff} which gives the impression that the entropy has increased even though the evolution is unitary.

To see how this comes about, write the complete density matrix in the form

$$\rho_{\text{out}} = \sum_i |c_i|^2 P(\Phi_i) \otimes P(\lambda_i) + \rho_{\text{int}}, \quad (117)$$

$$\rho_{\text{int}} = \sum_{i \neq j} c_i c_j^* (|\Phi_i\rangle \langle \Phi_j|) \otimes (|\lambda_i\rangle \langle \lambda_j|). \quad (118)$$

Interpretation

This chapter discusses the interpretation of quantum mechanics. That this basic topic has been postponed for so long, and that a whole chapter is being devoted to it, testifies to the unique character of quantum mechanics, for no text on a major topic in classical physics would have such a peculiar arrangement. The reason, of course, is that the mathematical structure of quantum mechanics is unfailingly successful in confronting an enormous range of phenomena, while the theory's epistemological framework does not have a clear link to the natural philosophy of classical physics and everyday life. As a consequence, the interpretation remains controversial. Furthermore, in our view it is easier to present and absorb a discussion of the interpretation of quantum mechanics when the formalism can be used without fear. To some minds, however, the formalism is a superfluous barrier to understanding



"I'd just like to know what in hell is happening, that's all! I'd like to know what in hell is happening! Do you know what in hell is happening?"

FIG. 12.1. ©2002 The New Yorker Collection from cartoonbank.com. All Rights Reserved.

Quantum Mechanics: Fundamentals

Gottfried, K.; Yan, T.-M.

2003, XVIII, 622 p., Softcover

ISBN: 978-0-387-22023-9